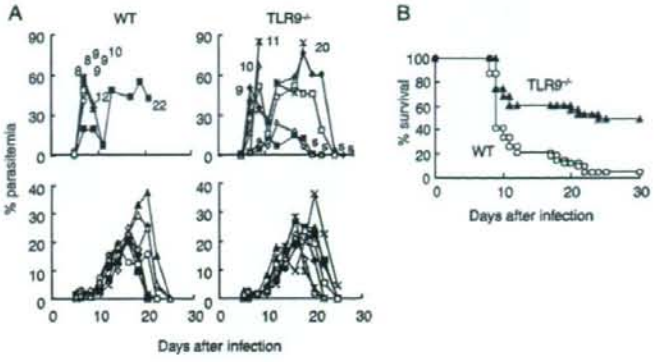

FIGURE 7. Resistance of TLR9$^{-/-}$ mice to PyL infection. *A*, The kinetics of parasitemia in WT or TLR9$^{-/-}$ mice infected with PyL (*upper panels*) or with PyNL (a nonlethal variant of PyL; *lower panels*) was monitored by microscopic evaluation of Giemsa-stained thin blood films. Each symbol represents a value from an individual mouse. The numbers represent days of mouse death and "s" shows mice that survived. Similar results were obtained from at least three experiments. *B*, The cumulative mortality rate of infection with PyL in WT (○) or TLR9$^{-/-}$ mice (▲) is shown. $p < 0.001$ for the percentage survival of WT vs TLR9$^{-/-}$ mice by χ^2 test.

To activate Tregs, phagocytosed pRBCs might not be displayed as Ags, but they were thought to provide signals to DCs. We hypothesized that TLRs are involved in this interaction. To investigate the possible roles of TLRs, we used DCs obtained from mice lacking MyD88 or TRIF, both of which are essential adaptor molecules for TLR signaling (21, 22). As shown in Fig. 6*A*, DCs from TRIF$^{-/-}$ mice were capable of activating Tregs as well as those from wild-type (WT) mice. By contrast, Tregs were not activated when cultured with DCs from MyD88$^{-/-}$ mice. The dependency of Treg activation on MyD88 and the endosomal localization allowed us to deduce that the TLRs likely to be involved are TLR7 and TLR9. TLR7 recognizes single-stranded RNA from viruses (23), while TLR9 recognizes DNA containing unmethylated CpG motifs (24). Recently, some reports have found that malaria parasites express molecules that are recognized by TLR9 (31, 32), suggesting that TLR9 is a much more likely candidate. To confirm this, we conducted studies using mice lacking TLR7 or TLR9. As expected, DCs from TLR7$^{-/-}$ mice, but not those from TLR9$^{-/-}$ mice, were able to activate Tregs (Fig. 6*B*). TLR9 is expressed predominantly by pDCs, which are reported to be involved in Treg induction (33). However, our experiments denied the involvement of pDCs in Treg activation during malaria infection. Purified PDCA1^{+} pDCs could not activate Tregs in vitro, presumably due to an inability to ingest pRBCs, whereas DCs depleted of pDCs could (Fig. 6*C*). These results indicate that TLR9 plays a critical role in the interaction between pRBCs and myeloid DCs, which underlies the activation of Tregs, and thus prompted us to examine the susceptibility of TLR9$^{-/-}$ mice to infection with PyL.

TLR9-deficient mice were partially resistant to lethal infection with PyL

As reported previously, rapid growth of the parasite occurred in WT mice, and these mice succumbed to infection within 2 wk (Fig. 7*A*); the overall mortality was >90% (30 of 32, Fig. 7*B*). Surprisingly, TLR9$^{-/-}$ mice were partially resistant to infection. Some mice were able to tolerate the second peak of parasitemia and ultimately survived, while other mice had only low levels of parasitemia (Fig. 7*A*). Cumulatively, 14 of 28 TLR9$^{-/-}$ mice survived (Fig. 7*B*). One possibility that needed to be excluded was that the WT mice died of hyperinflammation, such as CpG shock induced by the infection, and that the loss of TLR9 signaling merely reduced the immunopathology. Therefore, we measured the levels of proinflammatory cytokines in the sera of WT and TLR9$^{-/-}$ mice, but we were not able to detect IL-6, IL-12p70, or TNF-α, even after infection. The resistance of TLR9$^{-/-}$ mice was observed only when those mice were infected with PyL that activates Tregs. Infection of TLR9$^{-/-}$ mice with PyNL strain, which does not cause Treg activation, did not alter the course of infection (Fig. 7*A*). These results indicate that the loss of TLR9 might affect Treg activation but not immune responses unrelated to Treg activation.

Infection with PyL failed to activate Tregs in TLR9$^{-/-}$ mice

To relate the partial resistance against PyL infection to the impairment of Treg activation in TLR9$^{-/-}$ mice, we analyzed Treg function in TLR9$^{-/-}$ mice. Splenic Foxp3^{+}CD4^{+}CD25^{+} cells were increased in TLR9$^{-/-}$ mice, similarly to those in WT mice, 5 days

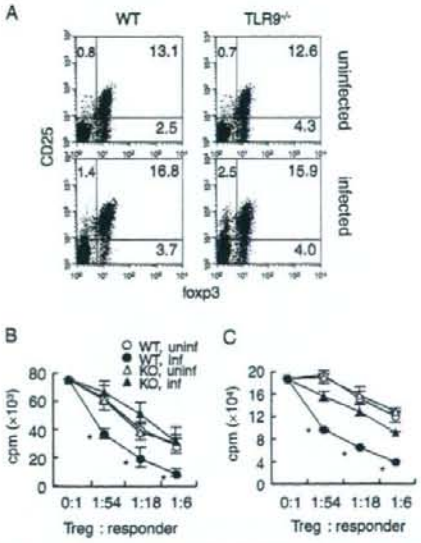

FIGURE 8. Impaired Treg activation in TLR9$^{-/-}$ mice after infection with PyL. *A*, Flow cytometric analysis of Foxp3 expression in CD4^{+}CD25^{+} T cells. Splenocytes obtained from WT (*left panels*) or TLR9$^{-/-}$ (*right panels*) mice with (*bottom panels*) or without (*top panels*) infection with PyL were analyzed as in Fig. 1*A*. Results are representative of five experiments. *B*, Suppressive function of Tregs in TLR9$^{-/-}$ mice infected with PyL. Splenic Tregs obtained from uninfected (open symbols) or PyL-infected (filled symbols), WT (circles) or TLR9$^{-/-}$ (triangles) mice were mixed with CD4^{+}CD25^{-} T cells at the indicated ratio. *C*, Transferred Ly5.1^{+} Tregs recovered from WT (circles) or TLR9$^{-/-}$ (triangles) recipients before (open symbols) or after (filled symbols) PyL infection were analyzed for their suppressive activity. Values are means ± SD of triplicate cultures. Asterisks indicate statistical significance at $p < 0.05$ with the Student t test. These experiments were repeated at least three times.

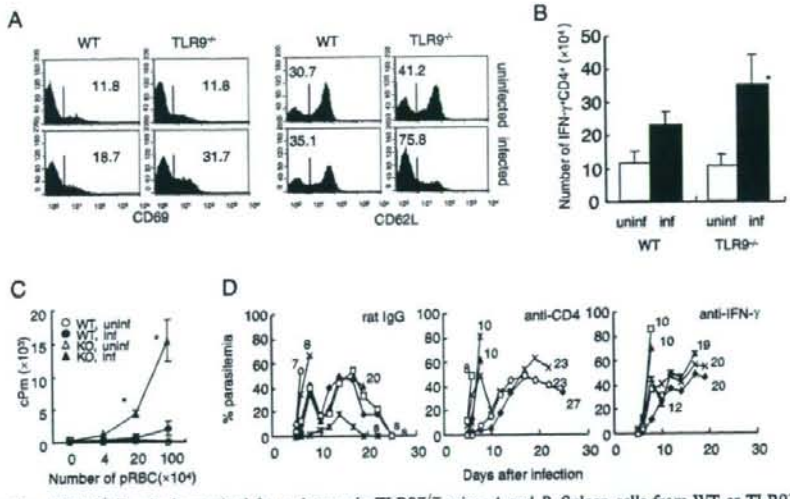

FIGURE 9. Activation of $CD4^+$ T cells is required for resistance in $TLR9^{-/-}$ mice. *A* and *B*, Spleen cells from WT or $TLR9^{-/-}$ mice 5 days after infection (*A*, *bottom panels*) or uninfected mice (*A*, *upper panels*) were stained with combinations of fluorescence-conjugated anti-CD4 and Abs to the indicated molecules, followed by flow cytometric analyses. *A*, Histograms show expression of CD69 or CD62L on gated $CD4^+$ T cells. Numbers indicate the percentages of $CD4^+$ T cells comprising the $CD69^{high}$ or $CD62L^{low}$ populations. *B*, The absolute number of $CD4^+IFN\text{-}\gamma^+$ cells in the spleen was calculated. Values are means ± SD of four mice. Asterisks indicate statistical significance at $p < 0.05$ with the Student *t* test. *C*, Proliferation of splenic $CD4^+$ T cells isolated from uninfected (open symbols) or PyL-infected (filled symbols) WT (circles) or $TLR9^{-/-}$ (squares) mice. $CD4^+$ T cells were cultured with the indicated number of pRBCs in the presence of APCs. Values are means ± SD of triplicate cultures. Asterisks indicate statistical significance at $p < 0.05$ with the Student *t* test. These experiments were repeated at least three times. *D*, $CD4^+$ T cells and IFN-γ are essential for protection against malaria parasites in $TLR9^{-/-}$ mice. The kinetics of parasitemia in $TLR9^{-/-}$ mice treated with the indicated Ab were evaluated as in Fig. 7*A*. Each symbol represents a value from an individual mouse. The numbers represent days to mouse death and "s" shows mice that survived. A similar result was obtained from another experiment.

after infection (Fig. 8*A*). Infection of WT mice with PyL again enhanced the suppressive function of Tregs, and infection of $TLR9^{-/-}$ mice failed to do so, although there was no difference in the suppressive efficacy between $TLR9^{-/-}$ and WT Tregs before infection (Fig. 8*B*). This failure might be attributable to the inclusion of $Foxp3^-$ cells among $CD4^+CD25^+$ cells, because $TLR9^{-/-}$ mice had more $CD4^+CD25^+Foxp3^-$ cells, which are thought to be effector cells originating from the pool of $CD4^+CD25^-$ cells (Fig. 8*A*). To exclude this possibility, we infected $TLR9^{-/-}$ mice into which Tregs from Ly5.1 mice had been adoptively transferred, and $Ly5.1^+$ cells recovered from the infected mice were analyzed for suppressive activity. $Ly5.1^+$ Tregs recovered from WT mice showed enhanced suppression after infection. By contrast, no enhancement of Treg function was observed in $TLR9^{-/-}$ recipients (Fig. 8*C*). These results confirm that Tregs are not activated in $TLR9^{-/-}$ mice, regardless of the expression of TLR9 on Tregs themselves.

Finally, we analyzed immune responses in PyL-infected $TLR9^{-/-}$ mice. $CD4^+$ T cells and their product IFN-γ are known to be important for protection against blood-stage malaria (34, 35). Flow cytometric analyses revealed that infection of $TLR9^{-/-}$ mice with PyL increased activated ($CD62L^{low}$, $CD69^{high}$) and $IFN\text{-}\gamma^+$ populations among splenic $CD4^+$ T cells, compared with infection of WT mice (Fig. 9, *A* and *B*). Furthermore, $CD4^+$ T cells from $TLR9^{-/-}$ mice proliferated in response to pRBCs, while those from WT mice showed only a marginal response (Fig. 9*C*). We depleted $CD4^+$ T cells or neutralized the IFN-γ from these mutant mice. These manipulations completely abolished the partial protection observed in $TLR9^{-/-}$ mice (Fig. 9*D*), indicating that $CD4^+$ T cells were efficiently activated under conditions in which Tregs are not activated in $TLR9^{-/-}$ mice.

Discussion

We herein demonstrate that malaria parasites activate Tregs through TLR9 engagement in DCs. PyL did not exert its full virulence in $TLR9^{-/-}$ mice, indicating that TLR9-mediated Treg activation is an important strategy used for immune escape by this parasite. The alterations observed in $TLR9^{-/-}$ mice, a failure of Treg activation and subsequent effector T cell activation, are dependent on TLR9-deficient DCs, because T cells, including Tregs, do not express TLR9 (17, 19). Among a variety of immune evasion mechanisms, DCs, which play central roles in establishing immunity, are the major target for malaria parasites. For instance, malaria parasites interfere with the maturation of DCs (3, 36, 37) or prevent Ag cross-presentation (38), both of which result in the failure to directly activate protective/effector T cells. Unlike these observations, our findings propose a novel interaction of malaria parasites with DCs via TLR9 that affects Tregs rather than protective T cells.

It is generally thought that TLRs are crucial for the induction of innate and acquired immunity (39). Some reports have shown that mice deficient in a TLR show higher susceptibility to pathogens recognized by the corresponding TLR (40, 41). By contrast, recent reports have shown TLR-mediated immune suppression. Upon stimulation through TLRs, on the one hand, DCs decrease the susceptibility of effector T cells to suppression mediated by Tregs (15). Stimulation of Tregs via TLR8 or TLR2 reverses the suppressive function of Tregs (17, 18). These behaviors drive toward the development of immunity. In contrast, systemic or excessive activation of TLRs in DCs has been reported to induce several types of immune suppression (38, 42). Stimulation with a large amount of LPS, a TLR4 ligand, and the TLR5 ligand flagellin

directly activate Tregs as determined by their enhanced suppressive function (19, 20). Thus, TLRs contribute to controlling the balance between Tregs and effector T cells by affecting both DCs and Tregs. Furthermore, TLR signaling provides negative feedback mechanisms for preventing immunopathogenesis when stimulation is saturated. Because TLR9 recognizes endogenous ligands and is involved in the development of autoimmune diseases (43, 44), this type of signal could have powerful regulatory functions, such as activation of Tregs, which are suppressors of autoimmunity. Indeed, TLR9 signaling plays a protective role in the development of autoimmunity by modulating Treg activity in autoimmune-prone MRL mice (45). Furthermore, common polymorphisms of TLR9 are reported to be associated with the clinical manifestation of malaria during pregnancy (46). It is quite possible that malaria parasites cleverly exploit this machinery by providing a large amount of TLR9 stimulant.

Recently it was reported that Tregs contribute to the pathogenesis of cerebral malaria by suppressing antimalarial immunity during infection with *Plasmodium berghei* ANKA (47). Tregs appeared to be activated in this model. It would be of interest to analyze whether TLR signaling is involved in this Treg activation, although the roles of TLRs in the development of cerebral malaria are controversial (48, 49).

Although we have not identified any TLR9 ligands derived from malaria parasites, the quantity of TLR9 signaling might be a key factor in the activation of Tregs. $TLR9^{+/-}$ heterozygous mice had a similar phenotype to $TLR9^{-/-}$ mice, but not to WT mice, in terms of a high resistance to malaria and an absence of Treg activation after infection (data not shown). Additionally, we postulate that the quality of parasite-derived TLR9 ligands is also important in the activation of Tregs for the following reasons. First, CpG-triggered DCs did not activate Tregs (data not shown). Second, stimulation of DCs with pRBCs did not induce production of IFN-α, which is secreted from DCs activated by CpG (data not shown). Given these findings, hemozoin, a known parasite ligand for TLR9, is a possible candidate ligand. Hemozoin is abundant in pRBCs, and it does not induce IFN-α production upon stimulation of DCs (31). Indeed, hemozoin-related immune suppression has been previously reported (50). Recently, the concept of malaria hemozoin stimulating TLR9 has been revised to malarial DNA presented by hemozoin (51). Careful investigations are required to identify the molecule(s) responsible for TLR9 stimulation.

Another issue to be clarified is how DCs that have interacted with malaria parasites activate Tregs. Infection of WT mice with PyL activated Tregs in terms of proliferation and suppressive functions. Cultivation of Tregs with DCs and pRBCs enhanced suppression, but did not induce proliferation. By contrast, infection of $TLR9^{-/-}$ mice increased the number of Tregs but did not enhance suppression. These results suggest that the regulation mechanisms for the augmentation of suppression might be different from those for proliferation. The failure of cultivation to increase the number of Tregs suggests that factors derived from other cell types, such as IL-2, are required for Treg proliferation. We postulate that parasite-simulated DCs up-regulate Foxp3 expression in Tregs, because flow cytometric analyses (Figs. 1*A* and 8*A*) show a slight increase in Foxp3 protein level in Tregs from infected mice, and because we found that the level of Foxp3 mRNA was increased in Tregs from mice infected with PyL (52). Ag-nonspecific augmentation of the suppressive activity of natural Tregs observed here has been reported after TLR5 ligation in human Tregs in vitro (20) or after infection of mice with helminth (53), both of which are associated with enhanced Foxp3 expression. TGF-β is important for Foxp3 expression, and both the increase in the number of $Foxp3^+$ Tregs and the production of TGF-β are associated with higher rates of parasite growth in human falciparum malaria (8), suggesting that TGF-β is likely to be responsible for Treg activation. However, our preliminary experiments showed that although the neutralization of TGF-β during PyL infection in mice augmented protective immunity, it did not attenuate Treg activation. Recently we found that malaria parasites induce DCs with a suppressive phenotype expressing IDO (54), which is known to be induced in DCs stimulated with systemic CpG injection (42). It would be interesting to analyze the involvement of this suppressive enzyme in Treg activation. Indeed, clarification of the molecular basis of Treg activation is our next objective.

In conclusion, we propose a novel model for the functional regulation of Tregs as well as for the immune escape of malaria parasites, which may enable us to establish new approaches to developing effective immunity against malaria or preventing autoimmunity by correcting the balance between Tregs and effector/pathogenic T cells.

Disclosures

The authors have no financial conflicts of interest.

References

1. Plebanski, M., K. L. Flanagan, E. A. M. Lee, W. H. H. Reece, K. Hart, C. Gelder, G. Gillespie, M. Pinder, and A. V. S. Hill. 1999. Interleukin 10-mediated immunosuppression by a variant CD4 T cell epitope of *Plasmodium falciparum*. *Immunity* 10: 651–660.
2. Smith, J. D., C. E. Chitnis, A. G. Craig, D. J. Roberts, D. E. Hudson-Taylor, D. S. Peterson, R. Pinches, C. I. Newbold, and L. H. Miller. 1995. Switches in expression of *Plasmodium falciparum var* genes correlate with changes in antigenic and cytoadherent phenotypes of infected erythrocytes. *Cell* 82: 101–110.
3. Urban, B. C., D. J. P. Ferguson, A. Pain, N. Willcox, M. Plebanski, J. M. Austyn, and D. J. Roberts. 1999. *Plasmodium falciparum*-infected erythrocytes modulate the maturation of dendritic cells. *Nature* 400: 73–77.
4. Sakaguchi, S., N. Sakaguchi, M. Asano, M. Itoh, and M. Toda. 1995. Immunologic self-tolerance maintained by activated T cells expressing IL-2 receptor alpha-chains (CD25): breakdown of a single mechanism of self-tolerance causes various autoimmune diseases. *J. Immunol.* 155: 1151–1164.
5. Shevach, E. M. 2002. $CD4^+CD25^+$ suppressor T cells: more questions than answers. *Nat. Rev. Immunol.* 2: 389–400.
6. Hori, S., T. L. Carvalho, and J. Demengeot. 2002. $CD25^+CD4^+$ regulatory T cells suppress $CD4^+$ T cell-mediated pulmonary hyperinflammation driven by *Pneumocystis carinii* in immunodeficient mice. *Eur. J. Immunol.* 32: 1282–1291.
7. Belkaid, Y., C. A. Piccirillo, S. Mendez, E. M. Shevach, and D. L. Sacks. 2002. $CD4^+CD25^+$ regulatory T cells control *Leishmania major* persistence and immunity. *Nature* 420: 502–507.
8. Hisaeda, H., Y. Maekawa, D. Iwakawa, H. Okada, K. Himeno Kishihara, S.-I. Tsukumo, and K. Yasutomo. 2004. Escape of malaria parasites from host immunity requires $CD4^+CD25^+$ regulatory T cells. *Nat. Med.* 10: 29–30.
9. Long, T. T., S. Nakazawa, S. Onizuka, M. C. Huaman, and H. Kanbara. 2003. Influence of $CD4^+CD25^+$ T cells on *Plasmodium berghei* NK65 infection in BALB/c mice. *Int. J. Parasitol.* 33: 175–183.
10. Walther, M., J. E. Tongren, L. Andrews, D. Korbel, E. King, H. Fletcher, R. F. Andersen, P. Bejon, F. Thompson, S. J. Dunachie, et al. 2005. Upregulation of TGF-β, FOXP3, and $CD4^+CD25^+$ regulatory T cells correlates with more rapid parasite growth in human malaria infection. *Immunity* 23: 287–296.
11. Setoguchi, R., S. Hori, T. Takahashi, and S. Sakaguchi. 2005. Homeostatic maintenance of natural $Foxp3^+CD25^+CD4^+$ regulatory T cells by interleukin (IL)-2 and induction of autoimmune disease by IL-2 neutralization. *J. Exp. Med.* 201: 723–735.
12. Marie, J. C., J. J. Letterio, M. Gavin, and A. Y. Rudensky. 2005. TGF-β1 maintains suppressor function and Foxp3 expression in $CD4^+CD25^+$ regulatory T cells. *J. Exp. Med.* 201: 1061–1067.
13. Yamazaki, S., T. Iyoda, K. Tarbell, K. Olson, K. Velinzon, K. Inaba, and R. M. Steinman. 2003. Direct expansion of functional $CD25^+CD4^+$ regulatory T cells by antigen-processing dendritic cells. *J. Exp. Med.* 198: 135–147.
14. Mahnke, K., Y. Qian, J. Knop, and A. H. Enk. 2003. Induction of $CD4^+CD25^+$ regulatory T cells by targeting of antigens to immature dendritic cells. *Blood* 101: 4862–4869.
15. Pasare, C., and R. Medzhitov. 2003. Toll pathway-dependent blockade of $CD4^+CD25^+$ T cell-mediated suppression by dendritic cells. *Science* 299: 1033–1036.
16. Kubo, T., R. D. Hatton, J. Oliver, X. Liu, C. O. Elson, and C. T. Weaver. 2004. Regulatory T cell suppression and anergy are differentially regulated by proinflammatory cytokine produce by TLR-activated dendritic cells. *J. Immunol.* 173: 7249–7258.
17. Peng, G., Z. Guo, Y. Kiniwa, K. S. Voo, W. Peng, T. Fu, D. Y. Wang, Y. Li, H. Y. Wang, and R.-F. Wang. 2005. Toll-like receptor 8-mediated reversal of $CD4^+$ regulatory T cell function. *Science* 309: 1380–1384.
18. Sutmuller, R. P. M., M. H. den Brok, M. Kramer, E. J. Bennink, W. L. Toonen, B.-J. Kullberg, L. A. Joosten, S. Akira, M. G. Netea, and G. J. Adema. 2006.

Toll-like receptor 2 controls expansion and function of regulatory T cells. *J. Clin. Invest.* 116: 485–494.
19. Caramalho, I., T. Lopes-Carvalho, D. Ostler, S., Zelenay, M. Haury, and J. Demengeot. 2003. Regulatory T cells selectively express Toll-like receptors and are activated by lipopolysaccharide. *J. Exp. Med.* 197: 403–411.
20. Crellin, N. K., R. V. Garcia, O. Hadisfar, S. E. Allan, T. S. Steiner, and M. K. Levings. 2005. Human $CD4^+$ T cells express TLR5 and its ligand flagellin enhances the suppressive capacity and expression of FOXP3 in $CD4^+CD25^+$ T regulatory T cells. *J. Immunol.* 175: 8051–8059.
21. Kawai, T., O. Adachi, T. Ogawa, K. Takeda, and S. Akira. 1999. Unresponsiveness of MyD88-deficient mice to endotoxin. *Immunity* 11: 115–122.
22. Yamamoto, M., S. Sato, H. Hemmi, K. Hoshino, T. Kaisho, H. Sanjo, O. Takeuchi, M. Sugiyama, M. Okabe, K. Takeda, and S. Akira. 2003. Role of adaptor TRIF in the MyD88-independent Toll-like receptor signaling pathway. *Science* 301: 640–643.
23. Diebold, S. S., T. Kaisho, H. Hemmi, S. Akira, and R. Sousa. 2004. Innate antiviral responses by means of TLR7-mediated recognition of single-stranded RNA. *Science* 303: 1529–1531.
24. Hemmi, H., O. Takeuchi, T. Kawai, T. Kaisho, S. Sato, H. Sanjo, M. Matsumoto, K. Hoshino, H. Wagner, K. Takeda, and S. Akira. 2000. A Toll-like receptor recognizes bacterial DNA. *Nature* 408: 740–745.
25. Hori, S., T. Nomura, and S. Sakaguchi. 2003. Control of regulatory T cell development by the transcription factor Foxp3. *Science* 299: 1057–1061.
26. Fontenot, J. D., M. A. Gavin, and A. Y. Rudensky. 2003. Foxp3 programs the development and function of $CD4^+CD25^+$ regulatory T cells. *Nat. Immunol.* 4: 330–336.
27. Ing, R., M. Segura, N. Thawani, N. Tam, and M. M. Stevenson. 2005. Interaction of mouse dendritic cells and malaria-infected erythrocytes: uptake, maturation, and antigen presentation. *J. Immunol.* 176: 441–450.
28. Germain, R. N. 1994. MHC-dependent antigen processing and peptide presentation: providing ligand for T lymphocyte activation. *Cell* 76: 278–289.
29. Barnden, M. J., J. Allison, W. R. Heath, and R. R. Carbone. 1998. Defective TCR expression in transgenic mice constructed using cDNA-based α- and β-chain gene under the control of heterologous regulatory elements. *Immunol. Cell Biol.* 76: 34–40.
30. Hori, S., M. Haury, A. Coutinho, and J. Demengeot. 2002. Specificity requirements for selection and effector function of $CD25^+4^+$ regulatory T cells in anti-myelin basic protein T cell receptor transgenic mice. *Proc. Natl. Acad. Sci. USA* 99: 8213–8218.
31. Pichyangkul, S., K. Yongvanitchit, U. Kum-arb, H. Hemmi, S. Akira, A. M. Krieg, D. G. Heppner, V. A. Stewart, H. Hasegawa, S. Looareesuwan, et al. 2004. Malaria blood stage parasites activate human plasmacytoid dendritic cells and murine dendritic cells through a Toll-like receptor 9-dependent pathway. *J. Immunol.* 172: 4926–4933.
32. Coban, C., K. J. Ishii, T. Kawai, H. Hemmi, S. Sato, S. Uematsu, M. Yamamoto, O. Takeuchi, S. Itagaki, N. Kumar, et al. 2005. Toll-like receptor 9 mediates innate immune activation by the malaria pigment hemozoin. *J. Exp. Med.* 201: 19–25.
33. Moseman, E. A., W. Liang, A. J. Dawson, A. Panoskaltsis-Mortari, A. M. Krieg, Y.-U. Liu, B. R. Blazar, and W. Chen. 2004. Human plasmacytoid dendritic cells activate by CpG oligodeoxynucleotides induce the generation of $CD4^+CD25^+$ regulatory T cells. *J. Immunol.* 173: 4433–4442.
34. Good, M. F., D. C. Kaslow, and L. H. Miller. 1998. Pathways and strategies for developing a malaria blood-stage vaccine. *Annu. Rev. Immunol.* 16: 57–87.
35. Matsumoto, S., H. Yukitake, H. Kanbara, and T. Yamada. 1998. Recombinant *Mycobacterium bovis* bacillus Calmette-Guerin secreting merozoite surface pfotein 1 (MSP1) induces protection against rodent malaria parasite infection depending on MSP1-stimulated interferon γ and parasite-specific antibodies. *J. Exp. Med.* 188: 845–854.
36. Ocana-Morgner, C., M. M. Mota, and A. Rodriguez. 2003. Malaria blood stage supperession of liver stage immunity by dendritic cells. *J. Exp. Med.* 197: 143–151.
37. Perry, J. A., C. S. Olver, R. C. Burnett, and A. C. Avery. 2005. Cutting edge: The acquisition of TLR tolerance during malaria infection impacts T cell activation. *J. Immunol.* 174: 5921–5925.
38. Wilson, N. S., G. M. N. Behrens, R. J. Lundie, C. M. Smith, J. Waithman, L. Young, S. P. Forehan, A. Mount, R. J. Steptoe, K. D. Shortman, et al. 2005. Systemic activation of dendritic cells by Toll-like receptor ligands or malaria infection impairs cross-presentation and antiviral immunity. *Nat. Immunol.* 7: 165–172.
39. Takeda, K., and S. Akira. 2003. Toll-like receptors. *Annu. Rev. Immunol.* 21: 335–376.
40. Bafica, A., C. A. Scanga, C. G. Feng, C. Leifer, A. Cheever, and A. Sher. 2005. TLR9 regulates Th1 responses and cooperates with TLR2 in mediating optimal resistance to *Mycobacterium tuberculosis*. *J. Exp. Med.* 202: 1715–1724.
41. Yarovinsky, F., D. Zhang, J. F. Andersen, G. L. Bannenberg, C. N. Serhan, M. S. Hayden, S. Hieny, F. S. Sutterwala, R. A. Flavell, S. Ghosh, and A. Sher. 2005. TLR11 activation of dendrtic cells by a protozoan profiling-like protein. *Science* 308: 1626–1629.
42. Wingender, G., N. Garbi, B. Schumak, F. Jungerkes, E. Endl, D. von Bubnoff, J. Steitz, J. Striegler, G. Moldenhauer, T. Tutting, et al. 2006. Systemic application of CpG-rich DNA suppresses adaptive T cell immunity via induction of IDO. *Eur. J. Immunol.* 36: 1–9.
43. Leadbetter, E. A., I. R. Rifkin, A. M. Hohlbaum, B. C. Beaudette, M. J. Shlomchik, and A. Marshal-Rothstein. 2002. Chromatin-IgG complexes activate B cell by dual engagement of IgM and Toll-like receptors. *Nature* 416: 603–607.
44. Barrat, F. J., T. Meeker, J. Gregorio, J. H. Chan, S. Uematsu, S. Akira, B. Chang, O. Duramod, and R. L. Coffman. 2005. Nucleic acids of mammalian origin can act as endogenous ligands for Toll-like receptors and may promote systemic lupus erythematosus. *J. Exp. Med.* 202: 1131–1139.
45. Wu, X., and S. L. Peng. 2006. Toll-like receptor 9 signaling protects against murine lupus. *Arthritis Rheum.* 54: 336–342.
46. Mockenhaupt, F. P., L. Hamann, C. van Gaertner, G. Bedu-Addo, C. von Kleinsorgen, R. R. Schumann, and U. Bienzle. 2006. Common polymorphisms of Toll-like receptors 4 and 9 are associated with the clinical manifestation of malaria during pregnancy. *J. Infect. Dis.* 194: 184–188.
47. Amante, F. A., A. C. Stanley, L. M. Randall, Y. Zhou, A. Haque, K. McSweeney, A. P. Waters, C. J. Janse, M. F. Good, G. R. Hill, and C. R. Engwerda. 2007. A role for natural regulatory T cells in the pathogenesis of experimental cerebral malaria. *Am. J. Pathol.* 171: 548–559.
48. Coban, C., K. J. Ishii, S. Uematsu, N. Arisue, S. Sato, M. Yamamoto, T. Kawai, O. Takeuchi, H. Hisaeda, T. Horii, and S. Akira. 2007. Pathological role of Toll-like receptor signaling in cerebral malaria. *Int. Immunol.* 19: 67–79.
49. Togbe, D., R. Schofield, G. E. Grau, B. Schnyder, V. Boissay, S. Charron, S. Rose, B. Beutler, V. F. J. Quesniaux, and B. Ryffel. 2007. Murine cerebral malaria development is independent of Toll-like receptor signaling. *Am. J. Pathol.* 170: 1640–1648.
50. Millington, O. R., C. Di Lorenzo, R. S. Phillips, P. Garside, and J. M. Brewer. 2006. Suppression of adaptive immunity to heterologous antigens during *Plasmodium* infection through hemozoin-induced failure of dendritic cell function. *J. Biol.* 5: 5.
51. Parroche, P., F. N. Lauw, N. Goutagny, E. Latz, B. G. Monks, A. Visintin, K. A. Halmen, M. Lamphier, M. Olivier, D. C. Bartholomeu, et al. 2007. Malaria hemozoin is immunologically inert but radically enhances innate responses by presenting malaria DNA to Toll-like receptor 9. *Proc. Natl. Acad. Sci. USA* 104: 1919–1924.
52. Hisaeda, H., S. Hamano, C. Mitoma-Obata, K. Tetsutani, T. Imai, H. Waldmann, K. Himeno, and K. Yasutomo. 2005. Resistance of regulatory T cells to glucocorticoid-induced TNFR-family related protein during *Plasmodium yoelii* infection. *Eur. J. Immunol.* 35: 3516–3524.
53. Wilson, M. S., M. D. Taylor, A. Balic, C. A. M. Finney, J. R. Lamb, and R. M. Maizels. 2005. Suppression of allergic airway inflammation by helminth-induced regulatory T cells. *J. Exp. Med.* 202: 1199–1212.
54. Tetsutani, K., H. To, M. Torii, H. Hisaeda, and K. Himeno. 2007. Malaria parasite induces tryptophan-related immune suppression in mice. *Parasitology* 134: 923–930.

Am. J. Trop. Med. Hyg., 79(6), 2008, pp. 819–822
Copyright © 2008 by The American Society of Tropical Medicine and Hygiene

Short Report: Concurrent Infection with *Heligmosomoides polygyrus* Modulates Murine Host Response against *Plasmodium berghei* ANKA Infection

Kohhei Tetsutani,* Kenji Ishiwata, Motomi Torii, Shinjiro Hamano, Hajime Hisaeda, and Kunisuke Himeno

Department of Parasitology, Kyushu University Graduate School of Medicine, Fukuoka, Japan; Department of Tropical Medicine, The Jikei University School of Medicine, Tokyo, Japan; Department of Molecular Parasitology, Ehime University School of Medicine, To-on, Ehime, Japan

Abstract. We investigated whether concurrent infection with *Heligmosomoides polygyrus*, an intestinal nematode, modulated anti-malaria parasite immunity and development of experimental cerebral malaria (ECM) in mice. The C57BL/6 mice infected with *Plasmodium berghei* ANKA showed typical symptoms of ECM. Interestingly, preceding *H. polygyrus* infection did not alter ECM development, despite accelerated *P. berghei* growth *in vivo*. Our observation provides a new insight that ECM can be induced in a fashion independent of the immune responses affected by concurrent *H. polygyrus*. Differentiation between protective immunity and infection-associated host-damaging inflammatory response is urgently required for understanding the pathogenesis of cerebral malaria.

Malaria parasites cause the worst parasitic disease, with hundreds of millions of clinical cases annually worldwide. Severe malarial anemia and cerebral malaria are of particular importance clinically, both of which are responsible for millions of deaths. Cerebral malaria is considered to be a consequence of mechanical occlusion of the small blood vessels in the brain with parasitized red blood cells (RBCs), and/or of immunologic pathology attributed to local inflammation.[1] Several lines of evidence supporting these hypotheses have been reported, yet the precise mechanisms underlying onset of cerebral malaria remain unclear.

A good rodent model for cerebral malaria is the infection of C57BL/6 mice with *Plasmodium berghei* ANKA, where the degree of immune activation reflects the extent of neurologic complications.[2] However, intestinal helminths cause the largest number of parasitic infections among humans, but they usually cause nil to mild symptoms during their chronic infections. It has been reported that host immune responses are modulated with intestinal helminthes. Infections with these helminths increase susceptibility to viral, bacterial, or parasitic infections, and attenuate efficacy of several vaccines against infectious diseases[3]; helminthic infections moderate allergic reactions or autoimmune conditions, which result from aberrant immune responses against foreign antigens or self-constituents.[3]

In humans, the prevalence of malaria and infections with intestinal helminths overlap geographically, and the population in a given area suffers from both infections.[4,5] It is supposed that infections with helminths affect the symptoms of malaria: Thai patients who have intestinal nematode infections suffer from malaria episodes more frequently.[6] Conversely, symptoms of each episode are less severe and the frequency of cerebral malaria, pulmonary edema, or renal failure, all of which are associated with immunopathology, is lower when patients have dense helminthic infections.[7]

It has been hypothesized that infections with intestinal helminths weaken protective immunity against co-existing malaria parasites, and simultaneously, the host-damaging inflammatory responses associated with malaria. To test this hypothesis, we examined the effects of concurrent infection with *Heligmosomoides polygyrus* on protective immunity and on experimental cerebral malaria (ECM) using C57BL/6 mice infected with *P. berghei*. All experiments using mice were conducted according to the guidelines for animal experimentation of Kyushu University.

Heligmosomoides polygyrus is a mouse intestinal nematode, which resides in the upper small intestine,[8] and it is maintained through *in vivo* passage using male ICR mice. For infection, feces containing eggs were incubated on wet filter paper for a minimum of three days to allow eggs to develop infective larvae. Male C57BL/6 mice at the age of eight to ten weeks were infected orally with 200 infective larvae by gastric intubation. Production of eggs began to be detected as early as 10 days after infection and continued for longer than eight weeks (data not shown). The mice did not show any central nervous system (CNS) symptoms during infection with *H. polygyrus*. After confirmation of *H. polygyrus* infection by feces examination, 2.5×10^4 *P. berghei*-infected RBCs were injected intraperitoneally (IP), at 14 days after *H. polygyrus* infection. Co-infection with *P. berghei* increased egg production by *H. polygyrus* slightly, without statistical significance (Figure 1).

Infection of C57BL/6 mice with *P. berghei* caused high lethality with CNS symptoms, which usually developed within

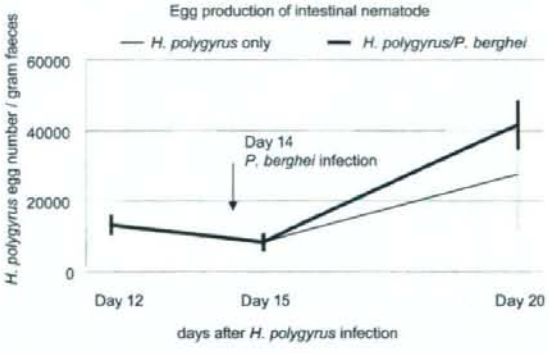

FIGURE 1. Egg production of *Heligmosomoides polygyrus*. The C57BL/6 mice were orally infected with infective larvae of *H. polygyrus*. Fecal egg number was counted at the indicated days after infection with *H. polygyrus*. Data show means ± SE of four to six mice. Experiments were repeated three times with similar results.

* Address correspondence to Kohhei Tetsutani, Department of Parasitology, Kyushu University Graduate School of Medicine, 3-1-1, Maidashi, Higashi-ku, Fukuoka, 812-0054, Japan. E-mail: tetztani@parasite.med.kyushu-u.ac.jp

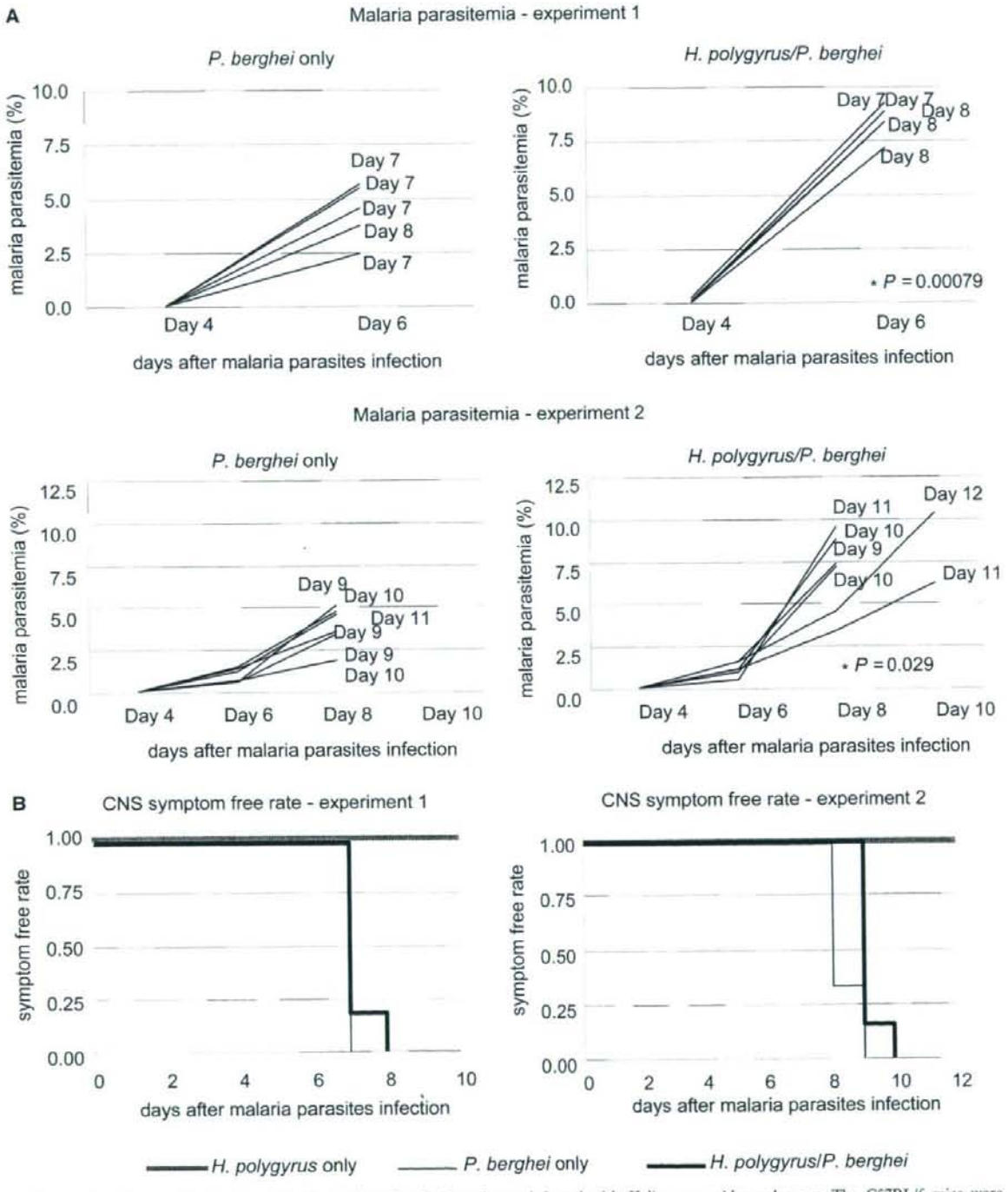

FIGURE 2. Course of infection with *Plasmodium berghei* in mice co-infected with *Heligmosomoides polygyrus*. The C57BL/6 mice were infected with *P. berghei* 14 days after *H. polygyrus* infection and were analyzed for percentage parasitemia monitored by microscopic evaluation of thin blood films stained with Giemsa solution (**A**), and for experimental cerebral malaria (ECM) incidence (**B**). Five to six animals were used in each group. Experiments were repeated three times with similar results and two of them are shown. (**A**) Each line represents data from an individual mouse, and the numbers indicate day of mouse death. An asterisk indicates statistical significance between mice infected with *H. polygyrus*/*P. berghei* and those only with *P. berghei* using the Student's *t* test. (**B**) *P. berghei*-infected animals were considered to have ECM when neurologic signs, described in the text, appeared. Statistical significance was not found between mice infected with *H. polygyrus*/*P. berghei* and those only with *P. berghei*.

10 days, despite a small parasite load in the circulation (Figure 2). *Heligmosomoides polygyrus*-infected mice showed significantly higher malaria parasitemia at the sixth to eighth day after infection (Figure 2A), which suggested that anti-malaria immunity might be suppressed, compared with the control mice infected only with *P. berghei*. But co-infected mice with *H. polygyrus* and *P. berghei* developed ECM similar to that in the control group, as evaluated by: 1) decrease in spontaneous activity; 2) loss of escape from handling; and 3) abnormal, non-abdominal body position (Figure 2B). Consequently, all mice died at around the tenth day, similar to the control mice (Figure 2A).

We observed here the rapid growth of *P. berghei* in mice co-infected with *H. polygyrus*, suggesting that concurrent *H. polygyrus* infection might have reduced anti-malaria immunity. Although we did not evaluate malaria–specific immune responses in these animals, our observations can be compatible with previous studies showing that *H. polygyrus*-harboring mice have suppressed both cellular and humoral immune responses against another rodent malaria, *Plasmodium chabaudi*.[9]

Although we have not addressed how *H. polygyrus* suppresses immunity, it has been postulated that protective Th1 responses are attenuated in the Th2-biased environment induced by concurrently infected *H. polygyrus*.[3] In addition to the classic Th1/2 balance, immunosuppressive mechanisms induced by *H. polygyrus* can explain the reduced protective immunity. *Heligmosomoides polygyrus* is now known to induce alternatively activated macrophages,[10] regulatory T cells,[11] interleukin-10, and indoleamine-2,3-dioxygenase (our unpublished observations). No matter what the mechanisms are, anti-malaria immunity is thought to be suppressed by *H. polygyrus* infection, which suggests that pathogenic processes formed by immune responses in ECM development are also attenuated.

There are some responses reported to participate in both protection and immunopathology: Interferon (IFN)-γ contributes not only to elimination of malaria parasites,[12] but also to the pathology of ECM.[13] Our preliminary results showed that *H. polygyrus* suppressed IFN-γ production from antigen–specific splenic T cells in mice after immunization with the corresponding antigen (unpublished observations). However unexpectedly, concurrent infection with *H. polygyrus* did not alter ECM development. This might be explained by the fact that immune suppression/modulation induced by concurrent *H. polygyrus* infection is not probably spread into CNS: *H. polygyrus* infection is reported to suppress experimental airway hypersensitivity,[14] although there have been no studies showing that nematodes whose life-cycle in their host are limited in alimentary tract to prevent experimental autoimmune/allergic encephalomyelitis (EAE) in CNS, although *Schistosoma mansoni*[15] and *Trichinella spiralis*,[16] which are thought to have easier access to the host blood stream, are reported to modulate EAE pathology. An alternative explanation is that protective immunity against malaria parasites is simply different from the pathogenic responses. For instance, although $CD8^+$ T cells are responsible for ECM development,[17] these cells are not supposed to contribute to protective immunity against blood-stage malaria parasites, mainly because of absence of MHC class I molecules on the surface of RBCs.[18] Finally, we cannot strictly exclude the probability that ECM pathology develops so quickly that modulations by concurrent *H. polygyrus* infection, if any, might not be obvious in our experiments. More sensitive methods of ECM diagnosis and definition are required for further research.

In conclusion, our results showed that infection with an intestinal nematode increased malaria parasite growth in vivo but did not alter immunopathology in ECM development. Differentiation between pathogen-killing immunity and self-damaging inflammatory responses is essential for a complete understanding of the pathology of cerebral malaria, and for designing effective vaccine strategies.

Received April 19, 2008. Accepted for publication August 20, 2008.

Financial support: This work was supported by the Ministry of Education, Science, Sport and Culture of Japan (Grants 20390121, 19041056), and by the Uehara Memorial Foundation.

Authors' addresses: Kohhei Tetsutani, Shinjiro Hamano, Hajime Hisaeda, and Kunisuke Himeno, Department of Parasitology, Kyushu University Graduate School of Medicine, 3-1-1, Maidashi, Higashi-ku, Fukuoka, 812-0054, Japan, Tel: +81-92-642-6117, Fax: +81-92-642-6118, E-mail: tetztani@parasite.med.kyushu-u.ac.jp. Kenji Ishiwata, Department of Tropical Medicine, The Jikei University School of Medicine, 3-25-8, Nishi-shinbashi, Minato-ku, Tokyo, Japan. Motomi Torii, Department of Molecular Parasitology, Ehime University School of Medicine, Shitsukawa, Toon, Ehime 791-0295, Japan.

REFERENCES:

1. van der Heyde HC, Nolan J, Combes V, Gramaglia I, Grau GE, 2006. A unified hypothesis for the genesis of cerebral malaria: sequestration, inflammation and hemostasis leading to microcirculatory dysfunction. *Trends Parasitol 22:* 503–508.
2. Medana IM, Chaudhri G, Chan-Ling T, Hunt NH, 2001. Central nervous system in cerebral malaria: "innocent bystander" or active participant in the induction of immunopathology? *Immunol Cell Biol 79:* 101–120.
3. van Riet E, Hartgers FC, Yazdanbakhsh M, 2007. Chronic helminth infections induce immunomodulation: consequences and mechanisms. *Immunobiol 212:* 475–490.
4. World Health Organization, 2004. Malaria cases (per 100,000) by country, latest available data. Available at: http://gamapserver.who.int/mapLibrary/Files/Maps/global_cases.jpg. Accessed April 8, 2008.
5. World Health Organization, 2006. Soil-transmitted helminth (STH) infections are widely distributed in tropical and subtropical areas – 2006. Available at: http://www.who.int/intestinal_worms/epidemiology/map/en/index.html. Accessed April 8, 2008.
6. Nacher M, Singhasivanon P, Yimsamran S, Manibunyong W, Thanyavanich N, Wuthisen P, Looareesuwan S, 2002. Intestinal helminth infections are associated with increased incidence of *Plasmodium falciparum* malaria in Thailand. *J Parasitol 88:* 55–58.
7. Nacher M, Gay F, Singhasivanon P, Krudsood S, Treeprasertsuk S, Mazier D, Vouldoukis I, Looareesuwan S, 2000. *Ascaris lumbricoides* infection is associated with protection from cerebral malaria. *Parasite Immunol 22:* 107–113.
8. Gause WC, Urban JF Jr, Stadecker MJ, 2003. The immune response to parasitic helminths: insights from murine models. *Trends Immunol 24:* 269–277.
9. Su Z, Segura M, Morgan K, Loredo-Osti JC, Stevenson MM, 2005. Impairment of protective immunity to blood-stage malaria by concurrent nematode infection. *Infect Immun 73:* 3531–3539.
10. Anthony RM, Urban JF Jr, Alem F, Hamed HA, Rozo CT, Boucher JL, van Rooijen N, Gause WC, 2006. Memory Th2 cells induce alternatively activated macrophages to mediate protection against nematode parasites. *Nat Med 12:* 955–960.
11. Finney CAM, Taylor MD, Wilson MS, Maizels RM, 2007. Expansion and activation of CD4+CD25+ regulatory T cells in

Heligmosomoides polygyrus infection. *Eur J Immunol 37:* 1874–1886.
12. Shear HL, Srinivasan R, Nolan T, Ng C, 1989. Role of IFN-γ in lethal and nonlethal malaria in susceptible and resistant murine hosts. *J Immunol 143:* 2038–2044.
13. Grau GE, Heremans H, Piguet PF, Pointaire P, Lambert PH, Billiau A, Vassalli P, 1989. Monoclonal antibody against interferon γ can prevent experimental cerebral malaria and its associated overproduction of tumour necrosis factor. *Proc Natl Acad Sci USA 86:* 5572–5574.
14. Wilson MS, Taylor MD, Balic A, Finney CAM, Lamb JR, Maizels RM, 2005. Suppression of allergic airway inflammation by helminth-induced regulatory T cells. *J Exp Med 202:* 1199–1212.
15. La Flamme AC, Ruddenklau K, Baecktroem BT, 2003. Schistosomiasis decreases central nervous system inflammation and alters the progression of experimental autoimmune encephalomyelitis. *Infect Immun 71:* 4996–5004.
16. Gruden-Movsesijan A, Ilic N, Mostarica-Stojkovic M, Stosic-Grujicic S, Milic M, Sofronic-Milosavljevic Lj, 2008. *Trichinella spiralis*: modulation of experimental autoimmune encephalomyelitis in DA rats. *Exp Parasitol 118:* 641–647.
17. Yanez DM, Manning DD, Cooley AJ, Weidanz WP, van der Heyde HC, 1996. Participation of lymphocyte subpopulations in the pathogenesis of experimental murine cerebral malaria. *J Immunol 157:* 1620–1624.
18. Vinetz JM, Kumar S, Good MF, Fowlkes BJ, Berzofsky JA, Miller LH, 1990. Adoptive transfer of CD8+ cells from immune animals does not transfer immunity to blood stage *Plasmodium yoelii* malaria. *J Immunol 144:* 1069–1074.

ELSEVIER

Journal of Hepatology 48 (2008) 237–245

Journal of Hepatology

www.elsevier.com/locate/jhep

Demonstration of cooperative contribution of MET- and EGFR-mediated STAT3 phosphorylation to liver regeneration by exogenous suppressor of cytokine signalings ☆,☆☆

Ekihiro Seki[1,2,3], Yuichi Kondo[1,2], Yuji Iimuro[1], Tetsuji Naka[4], Gakuhei Son[1], Tadamitsu Kishimoto[5], Jiro Fujimoto[1], Hiroko Tsutsui[6], Kenji Nakanishi[2,*]

[1]*Department of Surgery, Hyogo College of Medicine, Nishinomiya, Japan*
[2]*Department of Immunology and Medical Zoology, Hyogo College of Medicine, 1-1 Mukogawa-cho, Nishinomiya 663-8501, Japan*
[3]*Department of Medicine, University of California, San Diego, School of Medicine, CA 92093-0702, USA*
[4]*Department of Molecular Medicine, Osaka University Graduate School, Osaka, Japan*
[5]*Osaka University Graduate School, Osaka, Japan*
[6]*Department of Microbiology, Hyogo College of Medicine, Nishinomiya, Japan*

***Background/Aims*: As conditional knockout mice for *stat3* are impaired in liver regeneration after partial hepatectomy while those for *gp130* have defects in early STAT3 phosphorylation but have normal DNA synthesis, late STAT3 phosphorylation induced independently of gp130 seems to be essential for liver regeneration. Since HGF and EGF can activate STAT3 via gp130-independent MET and EGFR, respectively, we assumed that these factors account for STAT3-dependent liver regeneration. Here, we investigated this hypothesis by introducing suppressor of cytokine signaling (SOCS)-1 and SOCS3, potent negative regulators of STAT3 signaling, selectively in hepatocytes.**

***Methods*: We generated recombinant adenoviruses expressing *socs1* and *socs3*.**

***Results*: Hepatocytes infected with *socs1*-virus lacked STAT3 phosphorylation in response to IL-6 and HGF, while cells infected with *socs3*-virus lacked the response to all of IL-6, HGF and EGF, indicating that those SOCS proteins differently regulate EGFR signaling. Mice infected with *socs3*-virus exhibited severe and persistent impairment while those with *socs1*-virus showed only delayed regeneration, indicating requirement of both MET and EGFR signalings.**

***Conclusions*: These results clearly demonstrated that MET- and EGFR-mediated STAT3 signalings cooperatively contribute to liver regeneration and could provide new insights into tissue homeostasis.**

© 2007 European Association for the Study of the Liver. Published by Elsevier B.V. All rights reserved.

Keywords: **SOCS1; SOCS3; Adenovirus vector; ERK1/2; Hepatocyte**

Received 7 June 2007; received in revised form 20 July 2007; accepted 9 August 2007; available online 5 November 2007
Associate Editor: P.-A Clavien

☆ The authors declare that they do not have anything to disclose regarding conflict of interest with respect to this manuscript.

☆☆ This work was supported in part by Grants and a Hitec Research Center Grant from the Ministry of Education, Culture, Sports, Science and Technology of Japan and Collaborative Development of Innovation Seeds from Japan Science and Technology Agency in Japan.

* Corresponding author. Tel.: +81 798 45 6574; fax: +81 798 40 5423.
E-mail address: nakaken@hyo-med.ac.jp (K. Nakanishi).

Abbreviations: gp, glycoprotein; PHx, partial hepatectomy; SOCS, suppressor of cytokine signaling; JAK, Janus-activated kinase; moi, multiplicity of infection; Ab, antibody.

0168-8278/$32.00 © 2007 European Association for the Study of the Liver. Published by Elsevier B.V. All rights reserved.
doi:10.1016/j.jhep.2007.08.020

1. Introduction

Orchestrated activation of a signal network connecting cytokines, cell cycle transition, and growth factors is essential for homeostatic liver regeneration after liver resection or injury [1–3]. Immediately after liver resection or massive liver damage, nonparenchymal cells produce IL-6-related cytokines [1–6], and quiescent liver parenchymal cells start to replicate in response to various growth factors, such as HGF and EGF, via activating MET and EGFR, respectively [1–7]. These events converge into homeostatic liver regeneration. Conditional knockout mice for gene encoding glycoprotein (gp) 130, the common signaling component of receptors for IL-6-related cytokines, have severe defects in the early activation of STAT3 but are intact for DNA synthesis after partial hepatectomy (PHx) [8], indicating that gp130-mediated early STAT3 phosphorylation is dispensable for DNA synthesis. In contrast, conditional knockout mice for *stat3* have severe impairment in DNA synthesis [9], demonstrating the importance of STAT3 in the replication of hepatocytes. These observations allow us to assume that the early and late STAT3 phosphorylations in hepatocytes are induced by the gp130-dependent and -independent signalings, respectively, and that factors other than IL-6-related cytokines are essential for liver regeneration by inducing late STAT3 phosphorylation independently of gp130.

Suppressor of cytokine signaling (SOCS) is a family of intracellular molecules that negatively regulates various signal pathways [10–12]. SOCS1 and SOCS3 play their own roles in different biological situations by negatively regulating partially overlapped signal pathways [13–15]. SOCS1 binds to Janus-activated kinase (JAK) family members to negatively regulate various cytokine signalings, such as IL-6-induced STAT3 phosphorylation [13–16], while SOCS3 strongly interacts with activated cytokine receptors, such as gp130, to negatively regulate STAT3 phosphorylation [14–18]. Because HGF and EGF induced post PHx activate STAT3 via gp130-independent receptors, MET and EGFR, respectively [19–21], we assumed that MET- and EGFR-mediated signalings might account for the gp130-independent STAT3 phosphorylation. Here, we assessed this assumption by hepatocyte-selective introduction of SOCS1 and SOCS3. Infection of hepatocytes with recombinant adenoviruses expressing *socs1* only inhibited HGF-induced STAT3 phosphorylation, while those infected with recombinant virus expressing *socs3* could inhibit both EGF- and HGF-induced STAT3 phosphorylation. After PHx mice with exogenous SOCS3 exhibited persistently abolished DNA synthesis and liver mass restoration, those with ectopic SOCS1 expression showed only delay of these responses. These results indicated that absence of both MET- and EGFR-mediated STAT3 signalings almost completely abrogated liver regeneration and that absence of the MET-mediated STAT3 phosphorylation alone induces only slow-onset liver regeneration. These results demonstrated that the MET- and EGFR-mediated signalings cooperatively evoke liver regeneration process and shed light on the molecular mechanism for tissue homeostasis.

2. Experimental procedures

2.1. Mice

C57BL/6 mice were purchased from Clea Japan (Osaka, Japan). Six- to eight-week-old male mice were used. All mice were maintained under specific pathogen-free conditions, and received humane care as outlined in the Guide for the Care and Use of Experimental Animals in Hyogo College of Medicine.

2.2. Construction of recombinant adenovirus

Recombinant adenoviruses expressing genes encoding GFP (AxCA-GFP), murine SOCS1 (AxCA-SOCS1) and murine SOCS3 (AxCA-SOCS3), which contain a CAG promoter (chicken β-actin promoter with cytomegalovirus enhancer), were grown in 293 cells and prepared as shown previously [22]. AxCA-GFP was gifted from Dr. K. Ikeda at Osaka City University (Osaka, Japan). Viral titers were determined by optical densitometry (particles/ml) and by plaque-forming assay on HEK293 cells [22].

2.3. Adenovirus infection and operation procedure

Recombinant virus solution was injected (5×10^8 pfu in 0.2 ml) into mice via a tail vein (Supplementary Fig. 1A). At 48 h after infection, mice underwent 70% hepatectomy [4]. At the indicated time points after operation, serum and liver specimens were sampled. In some experiments, we measured the liver weight and calculated liver/body weight ratio [4]. Five to seven mice were used for each experimental group.

2.4. Hepatocyte preparation

Cells (5×10^5/ml) of hepatocytes were incubated with various adenoviruses at 50 of multiplicity of infection (moi) for 3 h [2]. The hepatocytes were incubated with recombinant murine IL-6 (20 ng/ml), EGF (20 ng/ml) or HGF (20 ng/ml) (R&D systems, Minneapolis, MN) for 15 min for detection of STAT3 phosphorylation. The culture medium generally used in this study is William E medium containing 15% FCS, 100 U/ml penicillin, 100 μg/ml streptomycin and 2 mM L-glutamine [23].

2.5. [^{3}H]-TdR incorporation assay

The hepatocytes were incubated with EGF (20 ng/ml) and HGF (20 ng/ml) for 48 h, during last 16 h with [^{3}H]-TdR, and incorporated [^{3}H]-TdR was counted [24]. Stimulation index was calculated as follows: Stimulation index = [^{3}H]-TdR incorporated in sample cells (cpm)/[^{3}H]-TdR incorporated in control cells (cpm).

2.6. Western blot analysis

Protein electrophoresis, protein transfer, and detection by Western blot were performed [4]. The primary Abs used were: anti-phosphotyrosine STAT3 Ab, anti-STAT3 Ab, anti-phospho ERK and anti-ERK from Cell Signaling (Beverly, MA), anti-cyclin D1 Ab (sc-717) (Santa Cruz Biotechnology, Santa Cruz, CA), and anti-SOCS1 Ab and anti-

SOCS3 Ab from IBL (Gumma, Japan). Secondary anti-rabbit or anti-mouse horseradish peroxidase-conjugated Abs were used at dilution of 1:2000 (Amersham Pharmacia Biotech, Piscataway, NJ).

2.7. Immunohistochemistry

BrdU analyses were performed as shown previously [4]. Liver specimens prepared from mice infected with AxCA-GFP 48 h before were fixed, frozen sections were incubated with rhodamine-conjugated anti-mouse F4/80 mAb (Biomedical AG, Augst, Switzerland), and immunofluorescence study was performed as shown previously [25].

2.8. Mitotic index

Liver sections were stained with hematoxylin and eosin, and mitotic hepatocytes in 30 high-power fields were counted. Average mitotic hepatocyte cell number in a high-power field was regarded as mitosis index [4].

2.9. Statistical analysis

All data are shown as means ± SD. Significance between control and experimental groups was examined with the unpaired Student's *t* test. *p* values less than 0.05 were considered significant. The representative data are shown. The similar results were obtained in two to three separate experiments.

3. Results

3.1. Exogenous SOCS1 and SOCS3 differentially regulate responses to HGF and EGF in hepatocytes

We generated recombinant adenoviruses expressing *socs1* and *socs3* in order to introduce those genes selectively in liver parenchymal cells [26]. First, we confirmed that infection with AxCA-SOCS1 and AxCA-SOCS3 is able to induce production of SOCS1 and SOCS3 proteins, respectively, in primary cultured hepatocytes in a dose-dependent manner (Fig. 1A). Hepatocytes infected with mock virus, AxCA-GFP, showed STAT3 phosphorylation upon stimulation with IL-6, while those infected with AxCA-SOCS1 or AxCA-SOCS3 exhibited abrogated STAT3 phosphorylation (Fig. 1B), indicating that exogenous SOCS1 and SOCS3 inhibit the gp130-mediated STAT3 phosphorylation.

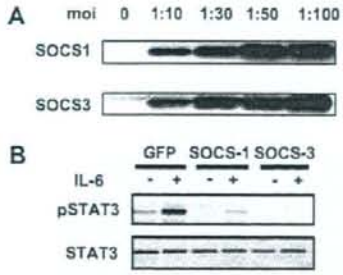

Fig. 1. Overexpressed *socs1* and *socs3* negatively regulate IL-6-induced STAT3 phosphorylation. (A) Primary cultured hepatocytes were incubated with AxCA-SOCS1 (SOCS1) or AxCA-SOCS3 (SOCS3). SOCS1 and SOCS3 protein levels were determined by immunoblotting. (B) Hepatocytes infected with AxCA-GFP (GFP), AxCA-SOCS1 or AxCA-SOCS3 were incubated with IL-6. Phosphorylated STAT3 (pSTAT3) or total STAT3 (STAT3) expressions were determined.

We wanted to know whether these exogenous SOCS proteins negatively regulate STAT3 phosphorylation in response to HGF or EGF. Hepatocytes infected with the mock virus showed STAT3 activation (Fig. 2A). By contrast, hepatocytes with ectopic expression of SOCS3 lacked STAT3 phosphorylation in response to both EGF and HGF (Fig. 2A), while those with ectopic *socs1* lacked it only in response to HGF but showed normal response to EGF (Fig. 2A), indicating that exogenous SOCS1 has narrowly limited target molecules as compared with SOCS3. Because both HGF and EGF can activate MAPK pathways [27,28], we analyzed ERK1/2 phosphorylation. HGF and EGF almost equiv-

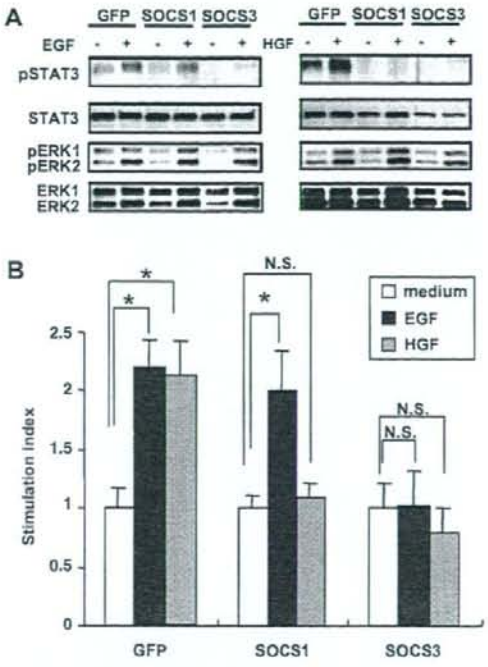

Fig. 2. Differentially impaired proliferative response to HGF and EGF in hepatocytes overexpressing SOCS1 and SOCS3. AxCA-GFP-, AxCA-SOCS1-, or AxCA-SOCS3-infected hepatocytes were incubated with HGF or EGF. Phosphorylated STAT3, total STAT3, phosphorylated (pERK1/2) and total ERK2 (ERK2) expressions were determined by immunoblotting (A). Primary cultured hepatocytes infected with AxCA-GFP, AxCA-SOCS1 or AxCA-SOCS3 were incubated with HGF or EGF and [^{3}H]-TdR incorporation in each experimental group was measured (B). Asterisks indicate $p < 0.05$. N.S. indicates not significant.

alently activated ERK1/2 in hepatocytes infected with all types of viruses (Fig. 2A), indicating that SOCS1 and SOCS3 proteins do not profoundly regulate the ERK1/2 phosphorylation.

Next, we investigated proliferative response to HGF and EGF. As expected, the mock virus-infected hepatocytes proliferated in response to HGF and EGF (Fig. 2B). By contrast, hepatocytes with exogenous SOCS3 failed to proliferate to both HGF and EGF, while the cells with excessive SOCS1 did not proliferate to HGF but could proliferate in response to EGF (Fig. 2B). Thus, there seems to be a positive correlation between STAT3 phosphorylation and DNA synthesis. Collectively, these results suggested that both SOCS1 and SOCS3 proteins inhibit hepatocyte proliferation by hampering the MET-mediated STAT3 activation and that only SOCS3 inhibits it by simultaneous abrogation of the EGFR-mediated STAT3 phosphorylation.

3.2. Exogenous SOCS1 or SOCS3 inhibits STAT3 phosphorylation but not ERK1/2 activation after PHx

Introduction of SOCS3 inhibits both MET- and EGFR-mediated STAT3 phosphorylation, suggesting SOCS3 inhibition of liver regeneration. Accordingly, we investigated whether the recombinant adenovirus introduces recombinant protein selectively in liver parenchymal cells. Those vectors preferred the liver to heart, lung, kidney and spleen (Supplementary Fig. 1B). Morphologically most of all GFP-positive cells are liver parenchymal cells (Fig. 3A). Immunohistochemistry for F4/80, a macrophage marker, on liver sections of mice infected with AxCA-GFP revealed that GFP-positive cells were primarily negative for F4/80 (Fig. 3B and C), demonstrating selective infection of liver parenchymal cells, but rarely Kupffer cells. These results indicated that the adenovirus is suitable to induce SOCS1 and SOCS3 proteins selectively in hepatocytes.

Next, we investigated whether exogenous SOCS1 and SOCS3 proteins influence STAT3 phosphorylation in the remnant liver after PHx. Consistent with our previous report [4], STAT3 was phosphorylated with peak around 2–6 h in control mice (Fig. 4A and B). This is also the case for the liver of mice infected with the control vector (Fig. 4A and B). By contrast, the early STAT3 activation was absent in AxCA-SOCS1- and AxCA-SOCS3-infected mice (Fig. 4A and B). The SOCS proteins were only detectable in the remnant liver homogenates prepared from mice infected with the individual *socs* viruses (Fig. 4A and B), although Northern blot analysis revealed the increased mRNA expressions in control mice (Supplementary Fig. 2). As the early STAT3 phosphorylation depends on gp130 [8], absence of these STAT3 phosphorylations in mice with ectopic expressions of SOCS proteins seemed to be due to the abrogated gp130-mediated STAT3 phosphorylation in hepatocytes (Fig. 1B).

Because MAPK pathway is also important for liver regeneration and is potently activated by both MET- and EGFR-mediated signals [27,29] we investigated whether exogenous SOCS1 and SOCS3 regulate this signal pathway. After PHx ERK1/2 phosphorylation was induced almost equivalently in mice with ectopic expression of *socs1* or *socs3* as in uninfected or the mock virus-infected control mice (Fig. 4C). Collectively, these results indicated that the introduction of SOCS1 or SOCS3 inhibits STAT3 activation, but not ERK phosphorylation, both *in vitro* (Fig. 2) and *in vivo* (Fig. 4).

Although IL-6 promptly induced after PHx is involved in the early STAT3 phosphorylation [1–3], there were no significant differences of increase in serum IL-6 among variously treated mice (Supplementary Fig. 3), indicating normal activation of the TLR/MyD88-signaling.

3.3. Impaired DNA synthesis in hepatocytes

Next, we investigated whether the enforced expression of SOCS1 or SOCS3 in hepatocytes inhibits their replication after PHx. To test this we counted BrdU-incorporated hepatocytes. Consistent with our previous reports [4], both uninfected and the mock virus-infected

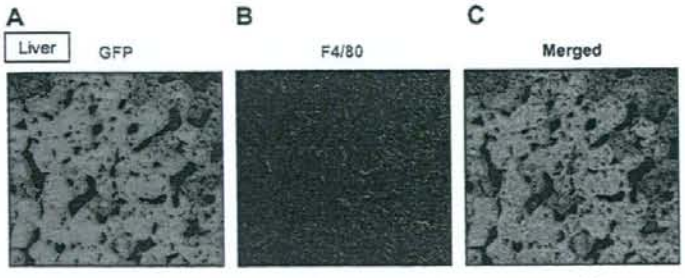

Fig. 3. Preferential infection of liver parenchymal cells with the vector virus. Mice were inoculated with 5×10^8 pfu of AxCA-GFP. Liver sections were incubated with rhodamine-labeled anti-F4/80. AxCA-GFP-infected cells are in green (A) and Kupffer cells are in red (B). (C) is a merged image of (A) and (B).

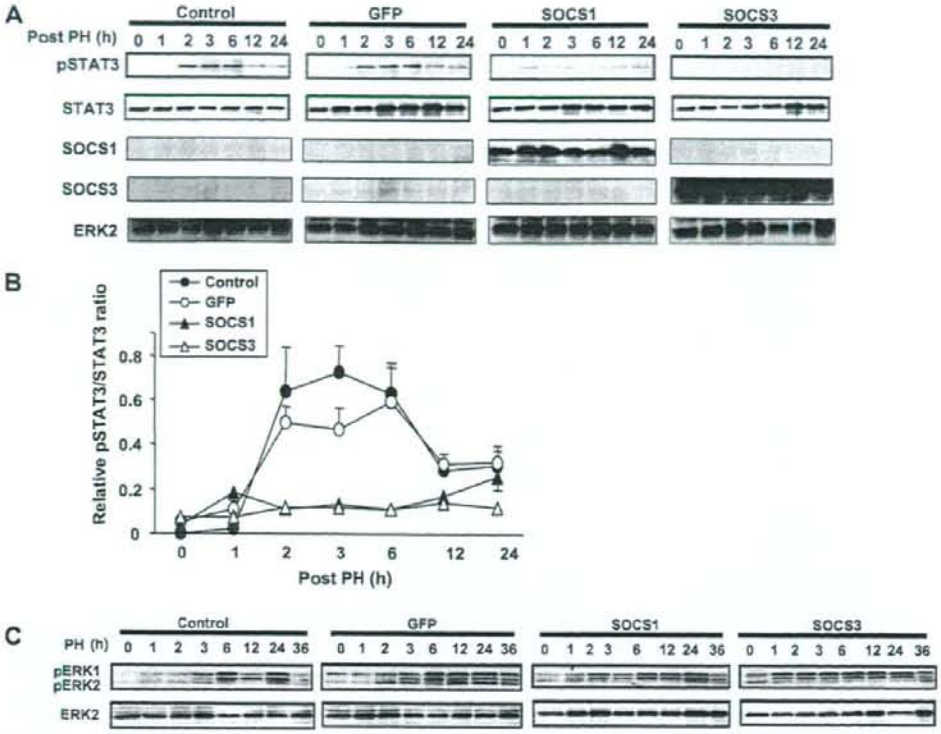

Fig. 4. Impaired STAT3 phosphorylation in mice overexpressing SOCS1 or SOCS3 after PHx. Mice were infected without (closed circles) or with AxCA-GFP (open circles), AxCA-SOCS1 (closed triangles) or AxCA-SOCS3 (closed triangles). (A and B) At the indicated time points after PHx, the remnant livers were removed. Phosphorylated, total STAT3, SOCS1 and SOCS3 were determined by immunoblotting (A). The individual image intensities were measured, and each relative pSTAT3/total STAT3 ratio was calculated (B). (C) At the indicated time points after PHx the remnant livers were removed. Phosphorylated and total ERK2 were determined by immunoblotting.

control mice showed increase in BrdU index (Fig. 5A and B). By contrast, AxCA-SOCS1- and AxCA-SOCS3-infected mice showed severe and complete impairment in increase of BrdU index, respectively (Fig. 5A and B), indicating that the hepatic introduction of *socs1* and *socs3* impairs DNA synthesis.

We also counted mitotic hepatocytes. The control mice showed an increase in mitosis index with a peak at 48 h (Fig. 5C–E). However, AxCA-SOCS1-infected mice exhibited severe impairment in mitotic index at 48 h but comparable index at 72 h as in control mice at 48 h (Fig. 5C–E), indicating that exogenous SOCS1 causes delay in hepatocyte mitosis. In agreement with the data of BrdU index (Fig. 5A and B), AxCA-SOCS3-infected mice had continuous abrogation of the hepatocyte mitotic responses (Fig. 5A–C), indicating that exogenous SOCS3 represses the hepatocyte mitosis. These results indicated that exogenous SOCS1 and SOCS3 cause the delay and the absence of DNA synthesis, respectively. Collectively, these results suggested that the recovery of DNA synthesis in AxCA-SOCS1-infected mice at a late phase is, at least partly, attributable to the normal EGFR-mediated signalings and that absence of both MET- and EGFR-mediated STAT3 signalings completely abrogates DNA synthesis.

3.4. Impaired cell cycle entrance

Since cell cycle progression is important for hepatocyte replication [1–3], we investigated the cell cycle entrance in the remnant liver of variously treated mice. We performed immunoblotting analyses for cyclin D1 that regulates the transition from G0/G1 to S phase [3]. Control or the mock virus-infected mice showed normal increase in cyclin D1 expression (Fig. 5E). However, cyclin D1 induction was seriously impaired in AxCA-SOCS1- and AxCA-SOCS3-infected mice at least until 72 h (Fig. 5E). These results indicated that the SOCS1 and SOCS3 proteins introduced inhibit cell cycle entrance after PHx.

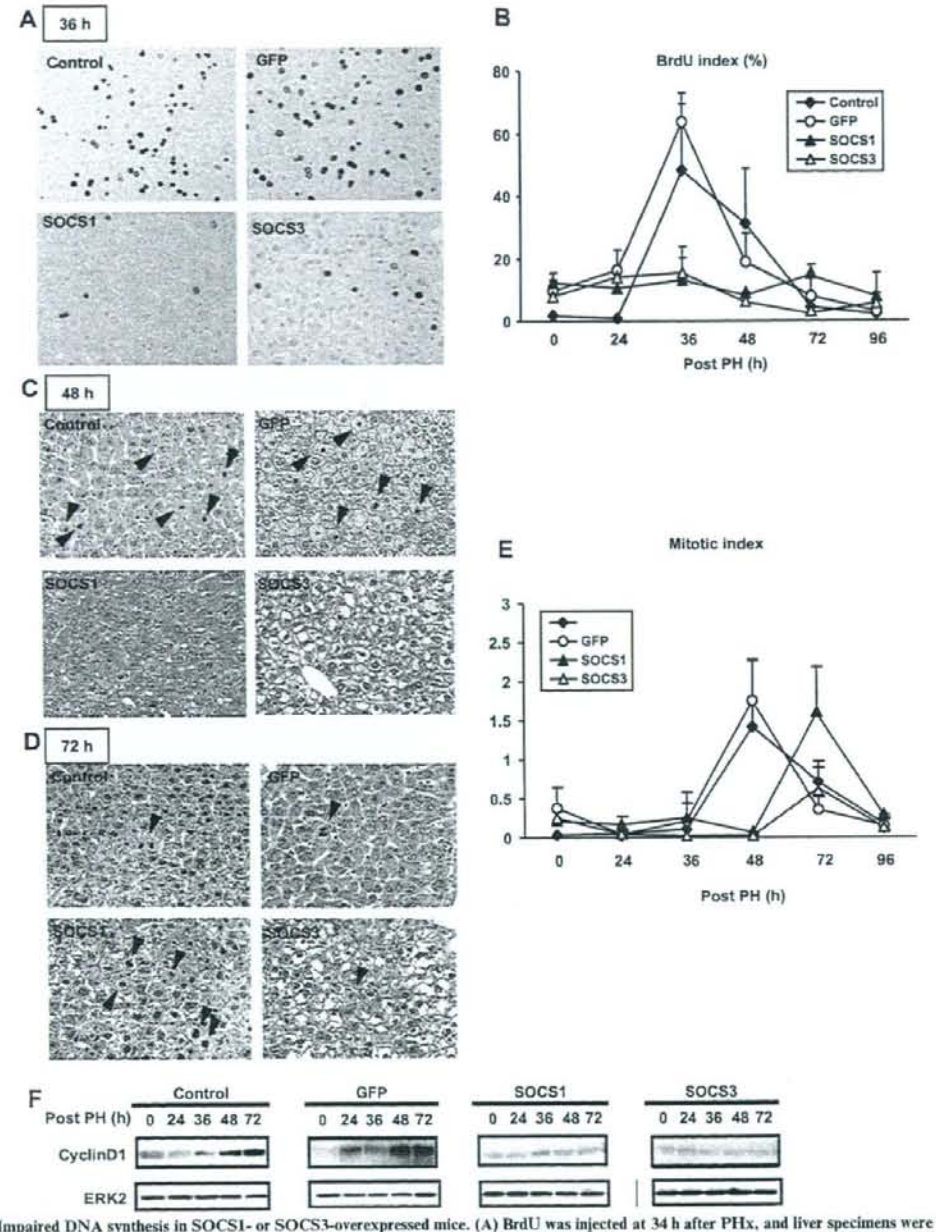

Fig. 5. Impaired DNA synthesis in SOCS1- or SOCS3-overexpressed mice. (A) BrdU was injected at 34 h after PHx, and liver specimens were sampled at 2 h later. BrdU-incorporated nuclei were stained in dark brown. Original magnification is 200×. (B) BrdU indices (percentage of BrdU-positive hepatocyte number to total hepatocyte number) were calculated in uninfected mice (closed diamonds; Control) or mice infected with AxCA-GFP (open circles), AxCA-SOCS1 (closed triangles) or AxCA-SOCS3 (open triangles) at the indicated time points after PHx. (C and D) Liver specimens were sampled at 48 h (C) or 72 h (D) after PHx. Original magnification is 200×. (E) Mitotic hepatocytes were numerically counted in uninfected mice (closed diamonds) or mice infected with AxCA-GFP (open circles), AxCA-SOCS1 (closed triangles) or AxCA-SOCS3 (open triangles) at the indicated time points after PHx, and mitotic indices were calculated. (F) The cyclin D1 and total ERK2 expressions, as a control protein, were determined by immunoblotting.

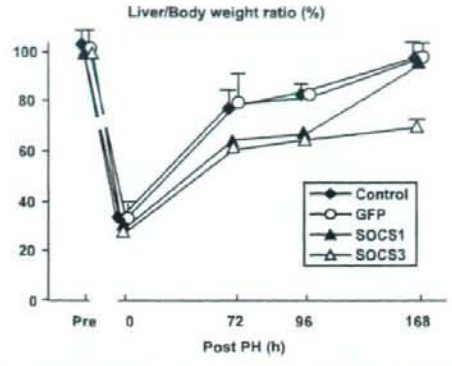

Fig. 6. Impaired liver mass restoration in SOCS1- or SOCS3-overexpressed mice. Livers were removed from uninfected (closed diamonds), or AxCA-GFP (open circles)-, -SOCS1 (closed triangles)-, -SOCS3 (open triangles)-infected mice at various time points after PHx, and percent liver/body weight ratio was calculated.

3.5. Impaired liver mass restoration

Finally, we examined whether these exogenous SOCS1 and SOCS3 in hepatocytes cause impairment in the liver mass restoration following PHx. Consistent with our previous work [4], the control mice recovered liver mass by day 7 (Fig. 6). Mice infected with AxCA-SOCS1 showed poor liver mass restoration until day 4 (Fig. 6). However, consistent with the result of DNA synthesis (Fig. 5A–E), full-blown liver mass restoration was observed at day 7 (Fig. 6). In agreement with the data of DNA synthesis (Fig. 5B and E), liver mass restoration was persistently impaired in AxCA-SOCS3-infected mice throughout the experimental course (Fig. 6). These results indicated that absence of the MET-mediated STAT3 signaling causes slow-onset liver mass restoration and that lack of both MET- and EGFR-mediated STAT3 signalings completely abolishes liver mass restoration.

4. Discussion

This is the first paper which clearly demonstrates that the MET- and EGFR-mediated STAT3 signalings cooperatively contribute to homeostatic liver regeneration. Exogenous SOCS3 negatively regulate both MET- and EGFR-mediated STAT3 phosphorylation and hepatocyte proliferation, while exogenous SOCS1 inhibited only MET- but not EGFR-mediated those responses (Fig. 2). As they selectively infect liver parenchymal cells (Fig. 3), these recombinant adenoviruses provide us with a powerful tool that can distinguish *in vivo* roles between MET- and EGFR-mediated signalings in liver regeneration. Consistent with the data of *in vitro* study (Fig. 1B), both mice overexpressing SOCS1 and those overexpressing SOCS3 failed to induce the early, gp130-mediated STAT3 phosphorylation (Figs. 4A and B and 7). However, both types of mice showed different outcomes in DNA synthesis and liver mass restoration. Mice with exogenous SOCS1 showed only delay in those responses, while those with exogenous SOCS3 exhibited complete impairments (Figs. 5A–E, 6 and 7). Hepatocytes of mice with exogenous SOCS3 showed different histology compared to control and SOCS1-overexpressing mice (Fig. 5), although the mechanism underlying is unclear. These results indicate that the absence of gp130- and MET-mediated STAT3 phosphorylations causes slow-onset DNA synthesis and that the late recovery of DNA synthesis in the former mice is, at least partly, due to their normal response to endogenous ligands for EGFR. By contrast, mice with exogenous SOCS3 showed continuous impairment in those responses due to their inability to activate all the gp130-, MET- and EGFR-mediated STAT3 signalings. These results, together with the article demonstrating

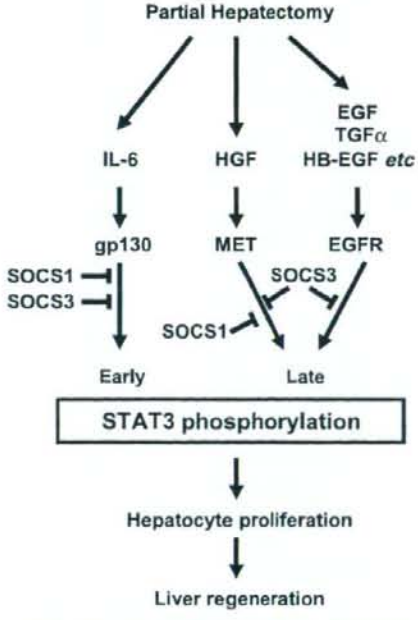

Fig. 7. Scheme for negative regulation of liver regeneration by ectopically expressed SOCS1 and SOCS3. Upon PHx, STAT3 is phosphorylated via gp130, MET, and EGFR by activation by the corresponding factors, such as IL-6-related cytokine, HGF, and EGF, TGF-α and HB-EGF, respectively, leading to liver regeneration. Exogenous SOCS1 negatively regulates gp130- and MET-mediated STAT3 phosphorylation but not EGFR signaling, resulting in delayed liver regeneration. By contrast, SOCS3 inhibited all of the signalings, leading to severely impaired liver regeneration.

the coordinated activation of EGFR and MET after PHx [7], indicated cooperative contribution of the gp130-, MET- and EGFR-mediated STAT3 signalings to normal liver regeneration.

Conditional knockout mice for *met* were reported to exhibit severe impairment in the liver regeneration following PHx or chemical liver injuries [30,31]. Intriguingly, $met^{-/-}$ mice showed persistently impaired liver mass restoration post PHx. In contrast, mice with ectopic expression of SOCS1 exhibited only delay in liver regeneration (Figs. 5 and 6). This discrepancy might be explained by the difference in activation of the MAPK signal pathways. $met^{-/-}$ mice showed persistent impairment in ERK1/2 phosphorylation [8], while mice infected with the *socs1* vector were intact for the ERK1/2 phosphorylation (Figs. 2A and 4C). These observations indicate that the complete absence of the MET-mediated signal pathways causes collapse of liver regeneration, while loss of single STAT3 activation produces only delay of it.

EGFR can recognize diverse growth factors for liver regeneration, including EGF, TGF-α, HB-EGF, and FGF family members [32,33]. It is conceivable that SOCS3 protein negatively regulates liver regeneration more powerfully than SOCS1 *in vivo* as well (Figs. 5 and 6).

A recent report showed that ectopic expressions of SOCS1 and SOCS3 inhibit STAT3 phosphorylation and migration of keratinocytes in response to HGF [34], supporting our present results (Fig. 2). It was reported that exogenous SOCS1 and SOCS3 bind to EGFR and negatively regulate EGFR/STAT3 signaling presumably by inducing ubiquitination-dependent EGFR degradation [35]. Indeed, introduction of *socs1* as well as *socs3* negatively regulates EGFR-mediated keratinocyte migration induced by antimicrobial peptide [36]. However, our present study revealed that exogenous SOCS3, but not SOCS1, negatively regulates the EGFR-mediated signaling (Fig. 2). These differences might be due to the cell types manipulated and to the EGFR ligands used.

It was reported that conditional knockout mice for STAT3 are impaired in DNA synthesis but have normal recovery of liver mass by compensatory hepatocellular hypertrophy [37]. Like the STAT3-deficient mice, mice overexpressing *socs1* and *socs3* showed impaired STAT3 activation (Fig. 4) and poor BrdU incorporation and mitoses (Fig. 5), but exhibited somewhat restoration of liver mass (Fig. 6). This might be due to the hypertrophy of liver parenchymal cells as well. Indeed, mice with *socs1* and *socs3* had the increase in size of hepatocytes compared to control mice (data not shown).

Our present results clearly demonstrate that both HGF- and EGF-induced STAT3 signalings are critical for the normal liver regeneration. Furthermore, these observations strongly indicate that hepatic SOCS1 and SOCS3 expressions are clinically beneficial criterion for liver resection with normal liver regeneration and may provide the possible precautionary and therapeutic regimen targeting SOCS1 and SOCS 3 [38–40] for the successful liver regeneration after liver resection.

Appendix A. Supplementary data

Supplementary data associated with this article can be found, in the online version, at doi:10.1016/j.jhep.2007.08.020.

References

[1] Taub R. Liver regeneration: from myth to mechanism. Nat Rev Mol Cell Biol 2004;5:836–847.
[2] Fausto N, Riehle KJ. Mechanisms of liver regeneration and their clinical implications. J Hepatobiliary Pancreat Surg 2005;2:181–189.
[3] Michalopoulos GK, Khan Z. Liver regeneration, growth factors, and amphiregulin. Gastroenterolology 2005;128:503–506.
[4] Seki E, Tsutsui H, Iimuro Y, Naka T, Son G, Akira S, et al. Contribution of Toll-like receptor/myeloid differentiation factor 88 signaling to murine liver regeneration. Hepatology 2005;41:443–450.
[5] Kishimoto T. Interleukin-6: from basic science to medicine-40 years in immunology. Annu Rev Immunol 2005;23:1–21.
[6] Streetz KL, Luedde T, Manns MP, Trautwein C. Interleukin 6 and liver regeneration. Gut 2000;47:309–312.
[7] Stolz DB, Mars WM, Petersen BE, Kim T-H, Michalopoulos GK. Growth factor signal transduction immediately after two-thirds partial hepatectomy in rat. Cancer Res 1999;59:3954–3960.
[8] Wuestefeld T, Klein C, Stretz KL, Bertz U, Lauber J, Buer J, et al. Interleukin-6/glycoprotein 130-dependent pathways are protective during liver regeneration. J Biol Chem 2003;278:11281–11288.
[9] Li W, Liang X, Kellendonk C, Poli V, Taub R. STAT3 contributes to the mitogenic response of hepatocytes during liver regeneration. J Biol Chem 2002;277:28411–28417.
[10] Naka T, Narazaki M, Hirata M, Matsumoto T, Minamoto S, Aono A, et al. Structure and function of a new STAT-induced STAT inhibitor. Nature 1997;387:924–929.
[11] Starr R, Willson TA, Viney EM, Murray LJL, Rayner JR, Jenkins BJ, et al. A family of cytokine-inducible inhibitors of signaling. Nature 1997;387:917–921.
[12] Endo TA, Masahara M, Yokouchi M, Suzuki R, Sakamoto H, Mitsui K, et al. A new protein containing an SH2 domain that inhibits JAK kinases. Nature 1997;387:921–924.
[13] Kubo M, Hanada T, Yoshimura A. Suppressors of cytokine signaling and immunity. Nat Immunol 2003;4:1169–1176.
[14] Alexander WS, Hilton DJ. The role of suppressors of cytokine signaling proteins in regulation of the immune response. Annu Rev Immunol 2004;22:503–529.
[15] Naka T, Fujimoto M, Tsutsui H, Yoshimura A. Negative regulation of cytokine and TLR signalings by SOCS and others. Adv Immunol 2005;87:61–122.
[16] Yoshimura A, Nishinakamura H, Matsumura Y, Hanada T. Negative regulation of cytokine signaling and immune responses by SOCS proteins. Arthritis Res Ther 2005;7:100–110.
[17] Yasukawa H, Ohishi M, Mori H, Murakami M, Chinen T, Aki D, et al. IL-6 induces an anti-inflammatory response in the absence of SOCS3 in macrophages. Nat Immunol 2003;4:551–556.

[18] Croker BA, Krebs DL, Zhang J-G, Wormald S, Willson TA, Stanley EG, et al. SOCS3 negatively regulates IL-6 signaling in vivo. Nat Immunol 2003;4:540–545.
[19] Bottaro DP, Rubin JS, Faletto DL, Chan AM, Kmiecik TE, Vande Woude GF, et al. Identification of the hepatocyte growth factor receptor as the c-met proto-oncogene product. Science 1991;251:802–804.
[20] Zhong Z, Wen Z, Darnell JEJ. Stat3: a STAT family member activated by tyrosine phosphorylation in response to epidermal growth factor and interleukin-6. Science 1994;264:95–98.
[21] Baccaccio C, Andò M, Tamagnone L, Bardelli A, Michieli P, Battistini C, et al. Induction of epithelial tubules by growth factor HGF depends on the STAT pathway. Nature 1998;391M:285–288.
[22] Iimuro Y, Nishiura T, Hellerbrand C, Behrns KE, Schoonhoven R, Grisham JW, et al. NF-κB prevents apoptosis and liver dysfunction during liver regeneration. J Clin Invest 1998;101:802–811.
[23] Adachi K, Tsutsui H, Kashiwamura S, Seki E, Nakano H, Takeuchi O, et al. *Plasmodium berghei* infection in mice induces liver injury by an IL-12- and Toll-like receptor/myeloid differentiation factor 88-dependent mechanism. J Immunol 2001;167:5928–5934.
[24] Schwabe RF, Bradham CA, Uehara T, Hatano E, Bennett BL, Schoonhoeven R, et al. c-Jun-N-terminal kinase drives cyclin D1 expression and proliferation during liver regeneration. Hepatology 2003;37:824–832.
[25] Ogushi I, Iimuro Y, Seki E, Son G, Hirano T, Hada T, et al. Nuclear factor κB decoy oligodeoxynucleotides prevent endotoxin-induced fatal liver failure in a murine model. Hepatology 2003;38:335–344.
[26] Lollo CP, Banaszczyk MG, Rill C, Coffin CC, Lucas MA, Chiou HC. Gene therapy strategies for the treatment of chronic viral hepatitis. Exp Opin Biol Ther 2001;1:629–639.
[27] Kermorgant S, Parker PJ. c-Met signalling. Cell Cycle 2005;4:352–355.
[28] Tarnowski AS. Cellular and molecular mechanisms of gastrointestinal ulcer healing. Dig Dis Sci 2005;50:S24–S33.
[29] Pierce KL, Luttrell LM, Lefkowitz RJ. New mechanisms in heptahelical receptor signaling to mitogen activated protein kinase cascades. Oncogene 2001;20:1532–1539.
[30] Huh CG, Factor VM, Sanchez A, Uchida K, Conner EA, Thorgeirsson SS. Hepatocyte growth factor/c-met signaling pathway is required for efficient liver regeneration and repair. Proc Natl Acad Sci USA 2004;101:4477–4482.
[31] Borowiak M, Garratt AN, Wustefeld T, Strehle M, Trautwein C, Birchmeier C. Met provides essential signals for liver regeneration. Proc Natl Acad Sci USA 2004;101:10608–10613.
[32] Breuhahn K, Longerich T, Schirmacher P. Dysregulation of growth factor signaling in human hepatocellular carcinoma. Oncogene 2006;25:3787–3800.
[33] Paranjpe S, Bowen WC, Bell AW, Nejak-Bowen K, Luo J-H, Michalopoulos GK. Cell cycle effects resulting from inhibition of hepatocyte growth factor and its receptor c-Met in regenerating rat livers by RNA interference. Hepatology 2007;45:1471–1477.
[34] Tokumaru S, Sayama K, Yamasaki K, Shirakata T, Hanakawa Y, Yahata Y, et al. SOCS3/Cis3 negative regulation of STAT3 in HGF-induced keratinocyte migration. Biophys Biochem Res Commun 2005;327:100–105.
[35] Xia L, Wang L, Chung AS, Ivanov SS, Ling MY, Dragoi AM, et al. Identification of both positive and negative domains within the epidermal growth factor receptor COOH-terminal region for signal transducer and activator of transcription (STAT) activation. J Biol Chem 2002;277:30716–30723.
[36] Tokumaru S, Sayama K, Shirakata Y, Komatuzawa H, Ouhara K, Hanakawa Y, et al. Induction of keratinocyte migration via transactivation of the epidermal growth factor receptor by the antimicrobial peptide LL-37. J Immunol 2005;175:4662–4668.
[37] Haga S, Ogawa W, Inoue H, Terui K, Ogino T, Igarashi R, et al. Compensatory recovery of liver mass by Akt-mediated hepatocellular hypertrophy in liver-specific STAT3-deficient mice. J Hepatol 2005;43:799–807.
[38] Shouda T, Yoshida T, Hanada T, Wakioka T, Oishi M, Miyoshi K, et al. Induction of the cytokine signal regulator SOCS3/CIS3 as a therapeutic strategy for treating inflammatory arthritis. J Clin Invest 2001;108:1781–1788.
[39] Yasukawa H, Yajima T, Duplain H, Iwatate M, Kido M, Hoshijima M, et al. The suppressor of cytokine signaling-1 (SOCS1) is a novel therapeutic target for enterovirus-induced cardiac injury. J Clin Invest 2003;111:469–478.
[40] Jo D, Liu D, Yao S, Collins RD, Hawiger J. Intracellular protein therapy with SOCS3 inhibits inflammation and apoptosis. Nat Immunol 2005;8:892–898.

Protective Effect of IL-18 on Kainate- and IL-1β-Induced Cerebellar Ataxia in Mice[1]

Tsugunobu Andoh,* Hiroyuki Kishi,[2†] Kazumi Motoki,[†] Kenji Nakanishi,[‡] Yasushi Kuraishi,* and Atsushi Muraguchi[†]

The pathogenesis of sporadic cerebellar ataxia remains unknown. In this study, we demonstrate that proinflammatory cytokines, IL-18 and IL-1β, reciprocally regulate kainate-induced cerebellar ataxia in mice. We show that systemic administration of kainate activated IL-1β and IL-18 predominantly in the cerebellum of mice, which was accompanied with ataxia. Mice deficient in caspase-1, IL-1R type I, or MyD88 were resistant to kainate-induced ataxia, while IL-18- or IL-18R α-deficient mice displayed significant delay of recovery from ataxia. A direct intracerebellar injection of IL-1β-induced ataxia and intracerebellar coinjection of IL-18 counteracted the effect of IL-1β. Our data firstly show that IL-18 and IL-1β display differential direct regulation in kainate-induced ataxia in mice. Our results might contribute toward the development of a new therapeutic strategy for cerebellar ataxia in humans. *The Journal of Immunology,* **2008, 180: 2322–2328.**

Kainate, an excitatory amino acid extracted from seaweed, has significantly contributed to understanding epileptogenesis (1). Previously, the effects of kainate on hippocampal neurons have been studied for delineating the mechanism of kainate-induced ataxia (1, 2). It is reported that L-glutamate, the major excitatory neurotransmitter in the brain, acts on three classes of ionotropic glutamate receptors: N-methyl-D-aspartate, α-amino-hydroxy-5-methyl-4-isoxazole propionic acid, and kainate receptors (3, 4). Kainate receptors consist of a set of genes (GluR5–7, KA-1, and KA-2), are widely distributed throughout the brain (5–10), and are implicated in epileptogenesis and neuronal cell death (11).

IL-1β and IL-18 are proinflammatory cytokines that are produced as a precursor form and proteolytically activated by caspase-1 (12). They are expressed in various tissues including the CNS (13–15). IL-1β is shown to exert neuroendocrine as well as neurodegenerative effects on animals (14, 15). It has been reported that convulsant stimuli increase the production of IL-1β and its receptor in rodent CNS within hours of seizure induction (16–18). Recently, Vezzani et al. reported that IL-1β prolongs hippocampal seizures in a N-methyl-D-aspartate receptor-dependent manner, and the action was inhibited by IL-1 receptor antagonist (IL-1ra)[3] (19, 20). Concerning IL-18, a crucial role for IL-18 in mediating neuroinflammation and neurodegeneration in the CNS under pathological conditions has been indicated (21).

Cerebellar ataxia, dysfunction of the cerebellum, causes problems such as loss of balance and motor coordination. Some types of cerebellar ataxia can be caused by several genetic mutations, including a group of autosomal dominant spinocerebellar ataxias (22) and autosomal recessive Ataxia telangiectasia (23); however, a large number of patients remain undiagnosed (sporadic cerebellar ataxias). In this study, we examined the roles of IL-1β and IL-18 in kainate-induced ataxia in mice. We demonstrated that IL-1β is activated specifically in the cerebellum by the systemic administration of kainate and is involved in kainate-induced ataxia in mice. Furthermore, we show that IL-18 in the cerebellum is involved in the recovery phase of kainate-induced ataxia by counteracting the function of IL-1β in the cerebellum. Our results show the possible anti-ataxic effect of IL-18 and may suggest new therapeutic strategies for cerebellar ataxia in humans.

Materials and Methods

Antibodies

Abs to GluR-5, GluR-6, IL-1β, IL-18, IL-1RI, calbindin, and glial fibrillary acidic protein were purchased from Santa Cruz Biotech; Abs to IL-18R and ST2L were purchased from R&D Systems; and an Ab to IL-33 were purchased from Alexa Biochem. Alexa488- or and Alexa564-conjugated anti-IgG were purchased from Molecular Probes.

Mice

Six- to 10-wk-old male mice were used in this study. BALB/c mice and C57BL/6 mice were purchased from Sankyo Laboratories. IL-1RI$^{-/-}$ mice with a C57BL/6 × 129 background and IL-18$^{-/-}$ mice with a C57BL/6 background were purchased from The Jackson Laboratory, and caspase-1$^{-/-}$ mice (24) with a BALB/c background, IL-18Rα$^{-/-}$ mice (25) with a C57BL/6 background, and MyD88$^{-/-}$ mice with a C57BL/6 background were provided by Dr. K. Kuida (Vertex Pharmaceuticals, Cambridge, MA) (24), Dr. T. Hoshino (Kurume University School of Medicine, Fukuoka, Japan) (25), and S. Akira (WPI Immunology Frontier Research Center, Osaka, Japan), respectively. These mice were maintained in our animal facility. Mice were housed under controlled temperature (23–25°C) and light (lights on from 08:00 h to 20:00 h) conditions. Food and water were freely available. The procedures for these animal experiments were reviewed and approved by the Committee for Animal Experiments at the University of Toyama.

*Department of Applied Pharmacology and †Department of Immunology, Graduate School of Medicine and Pharmaceutical Sciences, University of Toyama, Toyama, Japan; and ‡Department of Immunology and Medical Zoology, Hyogo College of Medicine, Nishinomiya, Japan

Received for publication September 11, 2007. Accepted for publication December 4, 2007.

The costs of publication of this article were defrayed in part by the payment of page charges. This article must therefore be hereby marked *advertisement* in accordance with 18 U.S.C. Section 1734 solely to indicate this fact.

[1] This work was supported by Grants in Aid for Scientific Research from the Ministry of Education, Culture, Sports, Science and Technology, Japan.

[2] Address correspondence and reprint requests to Dr. Hiroyuki Kishi, Department of Immunology, Graduate School of Medicine and Pharmaceutical Sciences, University of Toyama, 2630, Sugitani, Toyama, 930-0194 Japan. E-mail address: immkishi@med.u-toyama.ac.jp

[3] Abbreviations used in this paper: IL-1ra, IL-1 receptor antagonist; IL-1RI, IL-1 receptor type I.

Copyright © 2008 by The American Association of Immunologists, Inc. 0022-1767/08/$2.00

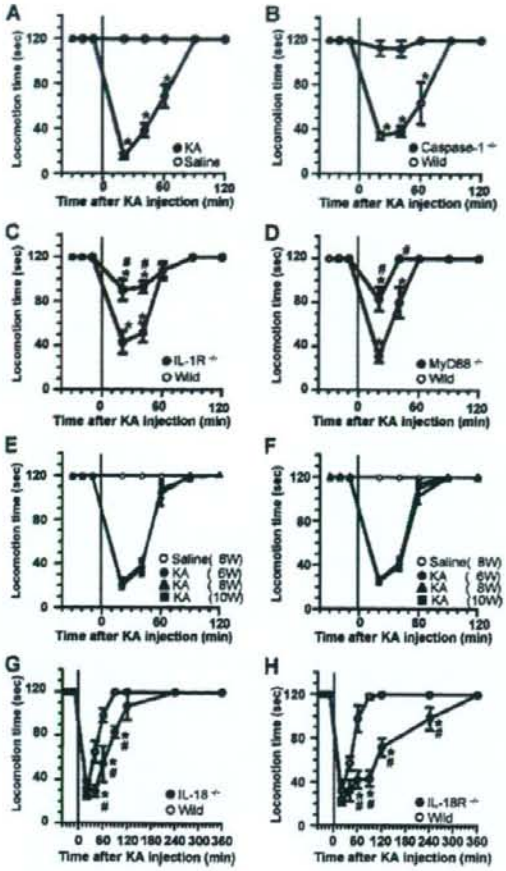

FIGURE 1. Deficiency with caspase-1, IL-1 receptor type I, or MyD88 attenuates the effect of kainate on inducing ataxia, but deficiency with IL-18 or its receptor delay the recovery from kainate-induced ataxia. *A*, Effect of kainate on locomotion activity in normal BALB/c mice was examined. Before kainate administration, a rotarod test was performed every 10 min (three times) and then kainate (KA) (20 mg/kg: ●) or saline (○) was i.p. injected into BALB/c mice at time 0. A rotarod test was performed at 20, 40, 60, 90, and 120 min after kainate injection. *, $p < 0.05$ when compared with average data before kainate injection ($n = 5$). *B–D*, *G*, and *H*, Effect of kainate on locomotion activity in wild-type mice vs gene-targeted mice was examined. A rotarod test was performed using (*B*) caspase-1$^{-/-}$ (●) or wild-type (○) mice, (*C*) IL-1RI$^{-/-}$ (●) or wild-type (○) mice, (*D*) MyD88$^{-/-}$ (●) or wild-type (○) mice, (*G*) IL-18$^{-/-}$ (●) or wild-type (○) mice, and (*H*) IL-18R$^{-/-}$ mice or wild-type (○) mice as mentioned above. *E* and *F*, Effect of kainate on locomotion activity in mice with different ages and genetic backgrounds was examined. A rotarod test was performed using either C57BL/6 mice (*E*) or BALB/c mice (*F*) 6- to 10-wk old. At time 0, kainate was injected. *, $p < 0.05$ when compared with the average data before kainate injection ($n = 5$). #, $p < 0.05$ when compared with wild-type mice ($n = 5$). Data are represented as the mean ± SEM.

Intracerebellar injection

Mice were lightly anesthetized with ethyl alcohol (wake up time: <20 s). The solution (0.5 μl) was injected into the center of the cerebellum using a 27G needle with a stopper held ~2 mm from the top of the needle and a microsyringe pump system.

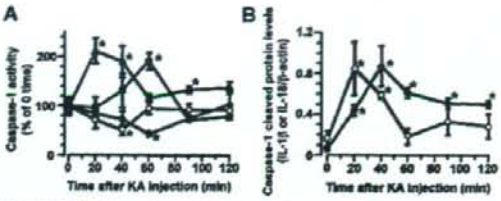

FIGURE 2. Systemic administration of kainate activates caspase-1, IL-1β, and IL-18 predominantly in cerebellum. Kainate (KA, 20 mg/kg) was i.p. injected into normal BALB/c mice and activity of caspase-1, IL-1β, and IL-18 was assessed. *A*, Activity of caspase-1 in cerebral cortex (○), cerebellum (△), hippocampus (■), and spinal cord (◆) was examined at various times after kainate-injection. Y-axis shows the percentage of caspase-1 activity compared with that at time 0. *, $p < 0.05$ when compared with the data at time 0 in each brain sample ($n = 4$). *B*, Caspase-1-processed protein levels of IL-1β and IL-18 in cerebellum were analyzed after systemic administration of kainate. Extracts from various parts of brain were separated on SDS-PAGE, and activated IL-1β (○) and IL-18 (●) were detected with immunoblotting. Y-axis shows the relative protein levels of activated IL-1β and IL-18 that are normalized with the protein level of β-actin ($n = 3$). Because significant levels of activated IL-1β and IL-18 were not detected in the cerebral cortex, hippocampus, and spinal cord, their data are omitted. Data are represented as the mean ± SEM.

Behavioral experiment

To estimate the effect of kainate and the other reagents on behavioral activity, a rotarod test was performed. To this end, Rota-Rod Treadmill (Ugo Basile) that consists of a gritted plastic rod flanked by two large round plates was used. Before performing the test, mice were trained on the rotarod until they reached a stable performance in this test (>120 s on rotarod) for one or two days before experiments. The test session was performed in accordance with the training session. Mice were brought to the experimental room at least 1 h before the experiment, and then placed on the accelerating rotarod apparatus (Ugo Basile Accelerating Rota-Rod "Jones & Roberts" for Rats 7750) with an initial speed of four rotations per

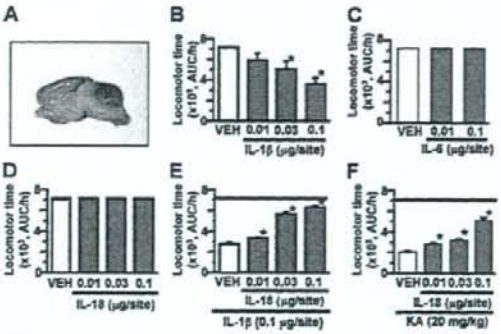

FIGURE 3. Intracerebellar injection of IL-1β induces ataxia, but intracerebellar injection of IL-18 together with IL-1β counteracted the effect of IL-1β in normal mice. *A*, Evans blue (0.5 μl) was intracerebellarly injected and its distribution was examined. *B–F*, Effect of intracerebellar injection of IL-1β, IL-18, or IL-6 on locomotion activity was examined. Various doses of IL-1β (*B*), IL-6 (*C*), IL-18 (*D*), or IL-18 with IL-1β (0.1 nmol/site) (*E*) were intracerebellarly injected and rotarod test was performed as mentioned in Fig. 1. *F*, Five min after intracerebellar injection of various doses of IL-18, kainate (KA, 20 mg/kg) was i.p. administered, and a rotarod test was performed. Y-axis shows the area under the curve (AUC) for 1 h after injection. *, $p < 0.05$ when compared with vehicle (VEH: saline)-treated group ($n = 5$). Dashed line shows the data from vehicle-treated group (*E*, without IL-1β; *F*, without kainate). Data are represented as the mean ± SEM.

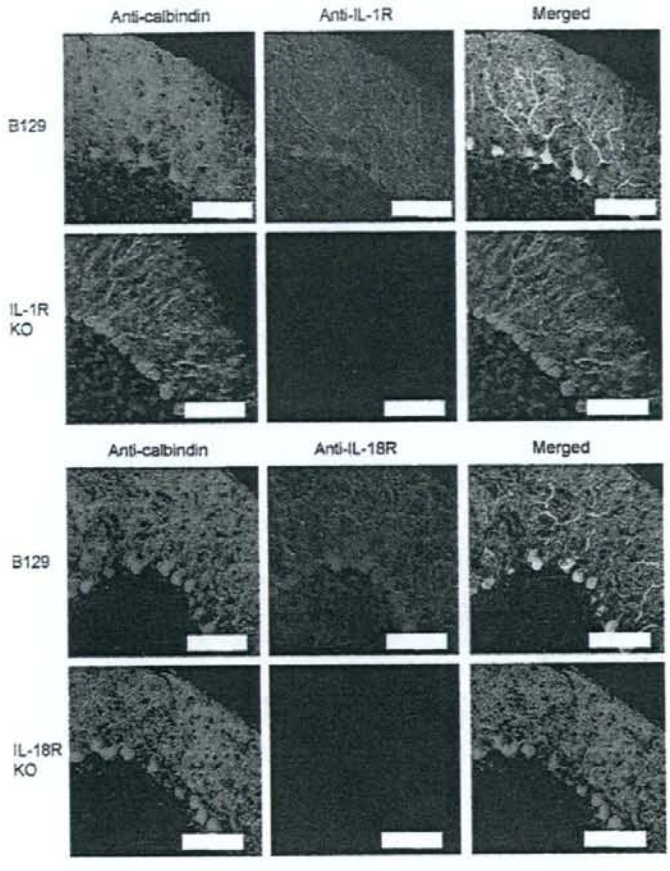

FIGURE 4. Immunohistochemical analysis of IL-1R and IL-18R in cerebellum is performed after the isolation of cerebellum from either normal mice, IL-1R$^{-/-}$ mice, or IL-18R$^{-/-}$ mice. The tissue section was stained with Ab to either IL-1RI or IL-18R, and then reacted with Alexa564-conjugated anti-rabbit or anti-goat IgG. To identify Purkinje cells, tissue sections were stained with Ab to calbindin, followed by Alexa488-conjugated anti-rabbit or anti-goat IgG. Fluorescent signals were detected using a confocal microscope. Scale bar, 100 μm.

minute; thereafter, the speed gradually increased to 60 rotations per minute. The time that the mouse remained on the rod was measured. A maximum of 120 s was allowed to test each animal. In the rotarod test, mice were pretreated with reagents or the vehicle, and the experiment was started 20 min after treatment.

Caspase-1 activity

Cell lysates were prepared by homogenizing the tissues (cerebral cortex, cerebellum, hippocampus, or spinal cord) in lysis buffer, centrifuged at 10,000 × *g* for 5 min at 4°C, and the supernatant was harvested. After determining the protein concentration, the cell lysates were used to measure the activity of caspase-1 using *N*-acetyl-Tyr-Val-Ala-Asp-*P*-nitroanilide as a substrate (Medical and Biological Laboratories). The reaction mixture was incubated for 2 h at 37°C. Caspase-1 activity was monitored with the absorbance at 420 nm, reacting chromophore *P*-nitroanilide.

Western blotting

Tissue samples (cerebral cortex, cerebellum, hippocampus, spinal cord) were homogenized in cell lysis buffer containing 137 mM NaCl, 20 mM Tris-HCl (pH 7.5), 1% Nonidet P-40, 10% glycerol, 1 mM PMSF, 10 μg/ml aprotinin, and 1 μg/ml leupeptin. The total protein concentration was determined using a Bio-Rad protein assay kit. Proteins were separated by electrophoresis using a 10 or 16% SDS-polyacrylamide gel and then transferred to a polyvinylidene fluoride membrane. The membrane was preincubated with a 5% skim milk solution for 1 h at room temperature, then incubated with primary Ab to either IL-1β or IL-18 at 4°C overnight, and subsequently incubated with a HRP-linked Ab against either mouse, rabbit, or goat IgG for 1 h. Membrane-bound HRP-labeled protein bands were reacted with a chemiluminescence detection solution (Amersham Biosciences). Chemiluminescent signals were detected using x-ray film. The amount of active IL-1β and IL-18 was evaluated by measuring the density of the active form cleaved by caspase-1 (17kD and 18 kD, respectively) using the National Institutes of Health Image program. The data were normalized with β-actin.

Immunohistochemistry

Mice were anesthetized with ethyl carbamate (1.5g/kg, i.p.) and perfused with 4% paraformaldehyde following PBS (pH 7.4). The mouse cerebellum was then isolated. The tissue was soaked in 4% paraformaldehyde for 4 h and then in 30% sucrose solution overnight at 4°C. A section (30 μm) was prepared using a cryostat. After washing with PBS, the section was soaked in PBS containing 0.3% Triton X-100 for 30 min and then in PBS containing 0.1% FBS for 30 min. The tissue section was incubated with the first Ab to either GluR-5, GluR-6, IL-1, IL-18, IL-1RI, IL-18R, calbindin, or glial fibrillary acidic protein overnight at 4°C, then washed with PBS, and reacted with Alexa488- or Alexa564-conjugated anti-IgG for 2 h. After washing with PBS, the sections were mounted with PBS/glycerol containing 0.05% triethylenediamine. Fluorescent signals were detected using a confocal microscope (Bio-Rad).

Data processing

All data are represented as the mean ± SEM. Statistical significance was analyzed using one-way ANOVA followed by Dunnett's multiple comparisons or Student's *t* test; $p < 0.05$ was considered significant.